# C H A P T E R 9

# ADVANCED SYSTEMS

## 9.1 Introduction

For decades the response to the ever-growing need for electric generation capacity was to build a new steam power plant, one not very different from the last. Today the energy conversion engineer is faced with a variety of issues and emerging technologies and a changing social and technological climate in which a diversity of approaches is likely to be accepted. This chapter intends to indentify some of these concerns and opportunities. No claim of completeness is made. No chapter, or book for that matter, could thoroughly cover this domain. The reader is referred to the bibliography at the end of the chapter as a starting point for continued study.

A few characteristics of importance in new power initiatives are: low capital and operating costs, ability to operate with a variety of fuels and with high tolerance to fuel variability, short construction time, low emission of pollutants, marketable or at least inert and easily disposable waste products, and high efficiency, maintainability, financeability, and reliability. Increasingly, the new initiative may take the form of repowering the the old plant so as to increase efficiency, meet pollution standards, and minimize the financial impact of meeting new power demands.

The improvement of the efficiency of power plants using conventional cycles is usually evolutionary in nature, by virtue of high temperature limitations and advances in materials. Hence, only gradual improvements in efficiency can be expected. On the other hand, significant improvements in efficiency can sometimes be obtained by combining conventional cycles in appropriate ways. Such power plants are referred to as *combined-cycle* plants. This chapter will examine the characteristics of several combined-cycle plants.

It is evident from the study of the Rankine and Brayton cycles, and in fact all heat engines, that the rejection of large amounts of thermal energy to the surroundings accompanies the production of useful power. This heat rejection can be reduced by improving the thermal efficiency of the cycle but cannot be eliminated. If this energy is not to be wasted, it is logical to seek applications where both power and rejected heat may be utilized. Power plants that produce mechanical or electrical power and utilize “waste heat” for industrial processes are called *cogeneration* plants. Several examples of cogeneration are considered in this chapter. District heating and other possible applications of waste heat are also discussed.

Another key problem facing the energy conversion engineer is the anticipated scarcity, in a few decades, of fuels such as natural gas and oil, relative to the vast resources of coal available in the United States and elsewhere. Perhaps future power plants should utilize this coal and nuclear energy to save the natural gas and

petroleum for industrial feedstocks and other more critical future needs. On the other hand, serious problems exist with respect to utilization of these resources. Nuclear power, an important alternative, replete with problems, is considered in the next chapter. Much of the readily available coal has unacceptably high sulfur, which significantly degrades the environment when released from power plant stacks in untreated combustion products. The well-known problem of acid rain has been attributed to emissions from coal-burning power plants. Thus the search for technology to utilize medium- and high-sulfur coal and to reduce levels of pollutant emissions of all types is an important area for research and development.

In this chapter advanced technologies that may contribute solutions to these and other crucial problems are considered. Some recent U.S. Department of Energy efforts in these areas may be found in Reference 66.

## 9.2 Combined-Cycle Power

One of the unfavorable characteristics of the gas turbine is that the exhaust gas issuing from the turbine is at high temperature, thereby wasting much energy and creating a local hazard. One solution to this problem was considered in Chapter 5: the addition of an exhaust gas heat exchanger to preheat the combustion air. The resulting regenerative cycle was found to be much more efficient than the corresponding simple cycle and to produce a lower exhaust gas temperature.

An alternative approach to dealing with the high gas turbine exhaust temperature is to provide a separate bottoming cycle to convert some of the energy of the turbine exhaust into additional power. Let's consider the use of a Rankine cycle that uses gas turbine exhaust as its energy source. It is clear that, if the Rankine cycle does not interfere with the operation of the gas turbine, the combined cycle will produce additional power and will have a higher efficiency than the gas turbine alone. Even if more heat is required for the Rankine bottoming cycle to produce additional work, the overall combined efficiency will increase if the additional work is large enough and supplemental heat small enough.

A combined gas turbine–Rankine cycle can be implemented in several ways. One method makes use of the fact that the exhaust of gas turbines usually has a high residual oxygen content because of the high air-fuel ratio required to limit the turbine inlet temperature when burning conventional fossil fuels. This hot, oxygen-rich exhaust gas can be used instead of air as the oxidizer in a steam generator as shown in Figure 9.1. For a moderate expenditure of additional natural gas in the furnace the resulting combustion products can provide heat for a high-temperature steam cycle with conventional steam plant technology.

The Horseshoe Lake combined-cycle plant was designed in this way to yield additional power and high efficiency when operating in the combined mode, and to operate with the gas turbine alone or with the steam turbine alone by direct-firing

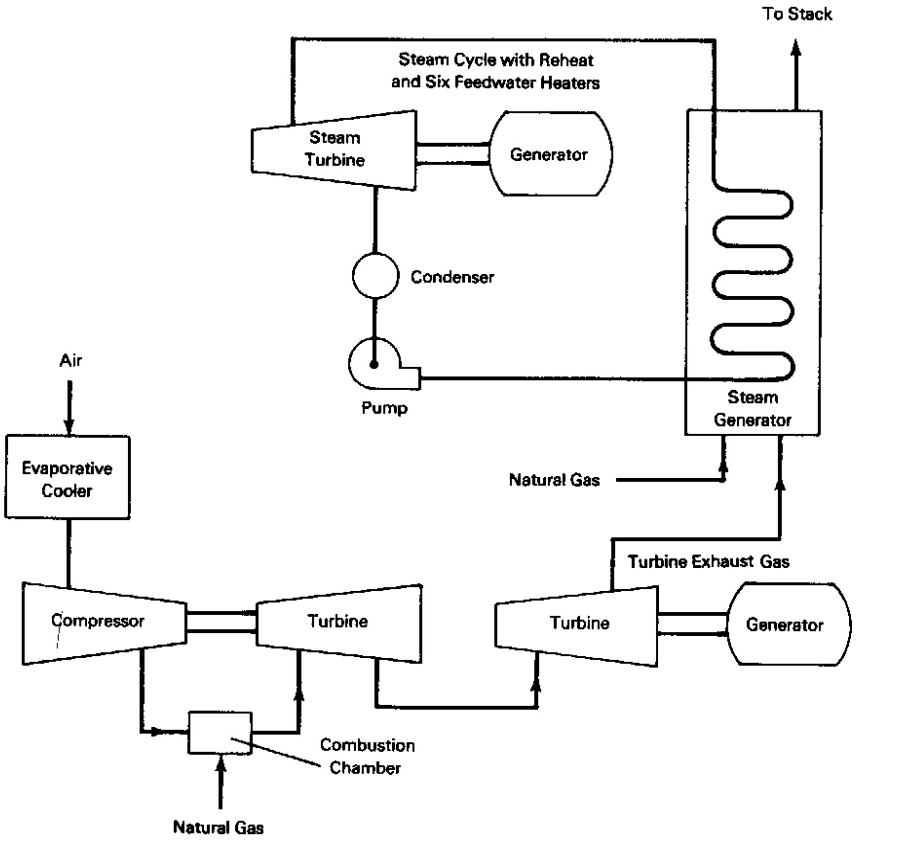


**FIGURE 9.1** Flow schematic of Horseshoe Lake combined-cycle plant.

of the steam generator with fuel and air. The plant, about ten miles east of

Oklahoma City, was the first its kind, first producing power in 1963. It was designed for a net output of 200 MW and a net heat rate of 9350 Btu/kW-hr. The plant cross-section and photos of the turbines are seen in Figures 9.2–9.4. Note the evaporative cooler to reduce the temperature and to increase the density of the air entering the gas turbine compressor. This reduces compressor work and increases inlet mass flow rate. Twenty years of successful operating experience with the Horseshoe Lake plant and information on similar German plants is documented in reference 46.

An open-cycle gas turbine also may be linked to a steam cycle through what may be considered a gas turbine exhaust heat exchanger containing an economizer, a boiler, and perhaps a superheater. This device, called a *heat-recovery steam generator* (HRSG), may be used to create and superheat steam as in a conventional steam cycle. A flow diagram for such a cycle is shown in Figure 9.5, together with a T-s diagram for the steam bottoming cycle. Gas turbine exhaust gas cools as it superheats, boils, and then warms liquid water in counterflow as it passes through the HRSG.

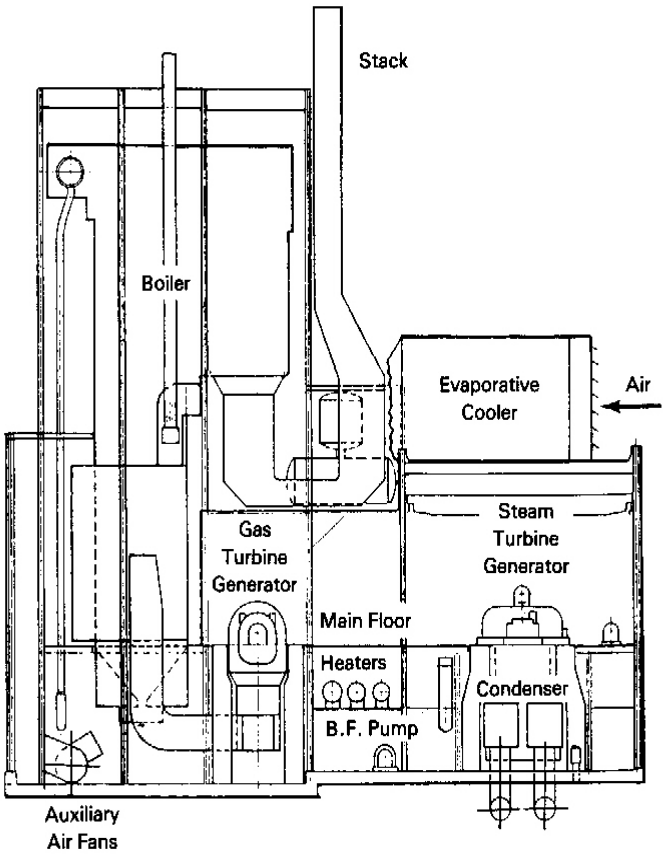


**FIGURE 9.2** Cross-section of the Horseshoe Lake plant. (Courtesy of Oklahoma Gas and Electric Co.)

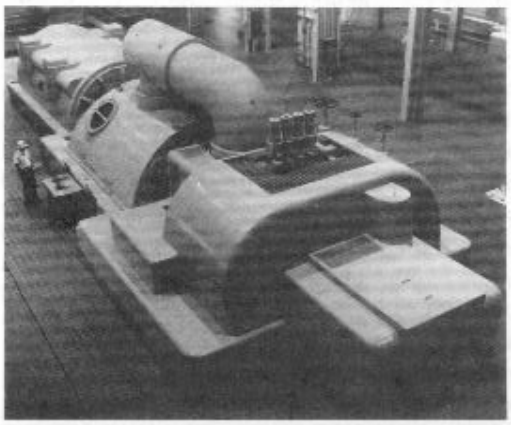

**FIGURE 9.3** Horseshoe Lake steam turbine. (Courtesy of Oklahoma Gas and Electric Co.)

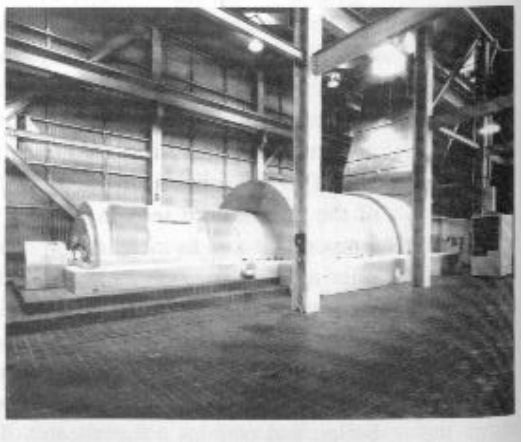

**FIGURE 9.4** Horseshoe Lake gas turbine. (Courtesy of Oklahoma Gas and Electric Co.)

**Combined-Cycle Analysis**

Assuming a constant heat capacity for the gas turbine combustion gas, we may compare gas temperatures with adjacent HRSG local water temperatures on the T-s diagram, Figure 9.5, by applying the steady-flow First Law of Thermodynamics to appropriate sections of the HRSG:

$$m_s(h_{12} - h_{11}) = m_g C_{pg}(T_6 - T_7) = m_s A_1 \qquad \text{[Btu/hr | kJ/hr]} \qquad (9.1)$$

$$m_s(h_{13} - h_{12}) = m_g C_{pg}(T_5 - T_6) = m_s A_2 \qquad \text{[Btu/hr | kJ/hr]} \qquad (9.2)$$

$$m_s(h_8 - h_{13}) = m_g C_{pg}(T_4 - T_5) = m_s A_3 \qquad \text{[Btu/hr | kJ/hr]} \qquad (9.3)$$

where $m_s$ and $m_g$ are the mass flow rates for the steam and gas turbine cycles, respectively, and the $A_i$ (i = 1, 2, 3) are the areas on the T-s diagram representing heat transfer per unit mass of steam. By adding the three equations, we obtain the same equation as would result from application of the steady-flow First Law of Thermodynamics to the entire HRSG:

$$\begin{aligned} m_s(h_8 - h_{11}) &= m_g C_{pg}(T_4 - T_7) \\ &= m_s(A_1 + A_2 + A_3) \end{aligned} \qquad \text{[Btu/hr | kJ/hr]} \qquad (9.4)$$

Thus the enthalpy rise of the steam in the HRSG is controlled by the ratio of mass flow rates and the hot-gas temperature drop. Expressing gas temperature in the HRSG in terms of steam enthalpy allows us to condense these equations into

$$T = T_7 + (m_s/m_g C_{pg})(h - h_{11}) \qquad \text{[R | K]} \qquad (9.5)$$

It is evident that the gas temperature is linearly proportional to the water enthalpy on a T-h diagram, as shown in Figure 9.6. The abscissa may be viewed as the cumulative heat transfer per unit mass of water, which is in turn proportional to the exhaust gas heat transfer.

The temperature difference $T_6 - T_{12}$, known as the *pinchpoint temperature difference*, is at a critical location in the heat recovery steam generator, because it occurs at the point of minimum temperature difference between the two fluids. It should exceed some minimum design value (about 30°F) for all operating conditions of the system to make effective use of all of the HRSG heat transfer surface. Smaller temperature differences would substantially increase the heat transfer surface area needed, while significantly larger values would necessitate reducing the boiling temperature and would adversely affect the combined-cycle thermal efficiency.

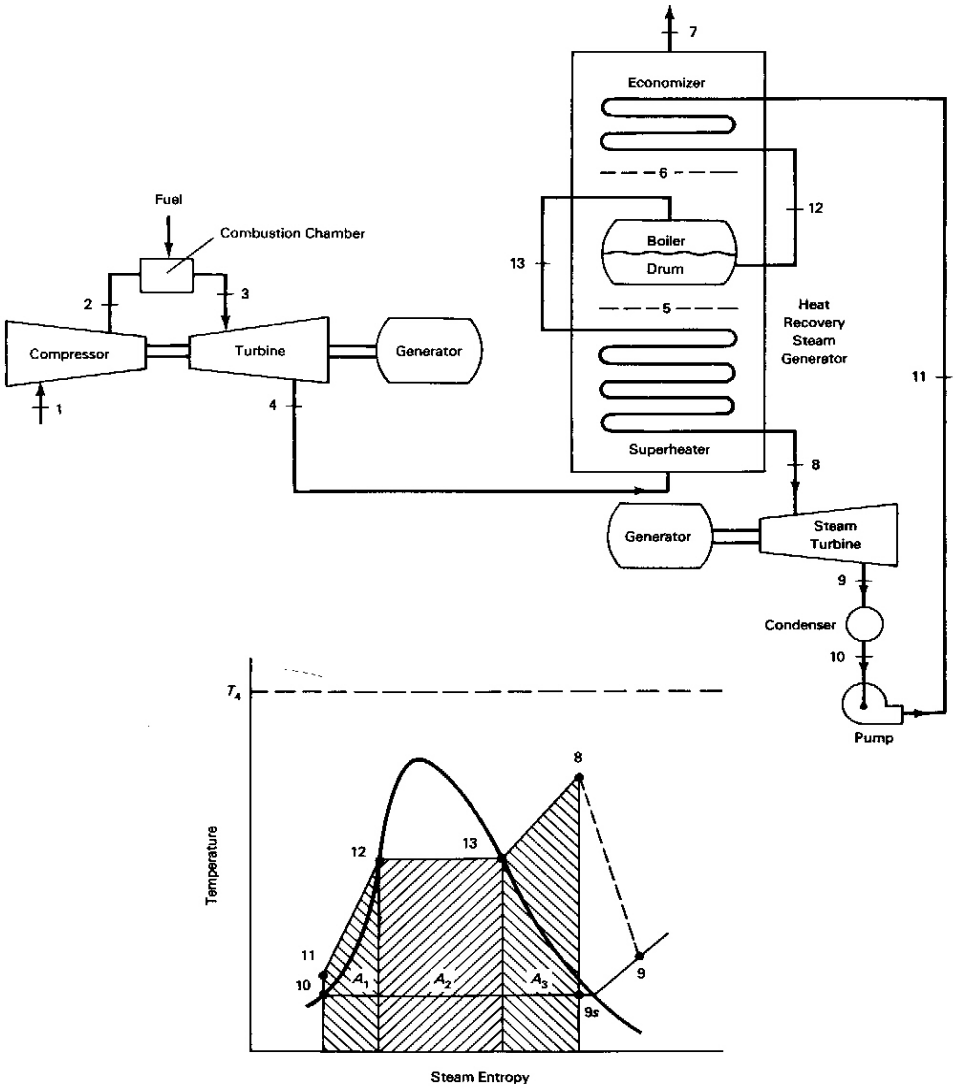


**FIGURE 9.5** Combined-cycle gas and steam turbines using an unfired heat-recovery steam generator.

## EXAMPLE 9.1

Let us examine several possible Rankine bottoming cycles for the gas turbine considered earlier in Example 5.1. There a gas turbine with a compressor pressure ratio of 6 and a turbine inlet temperature of 1860°R was analyzed. The turbine exhaust temperature was found to be 1273°R, or 813°F. With 813°F as the HRSG gas entrance temperature, select the steam turbine throttle temperature as 700°F and consider Rankine cycles with a range of boiling temperatures, a condensing temperature of 100°F, and a pinchpoint temperature difference of at least 30°F. Determine a cycle with a satisfactory boiling temperature, and compare it with

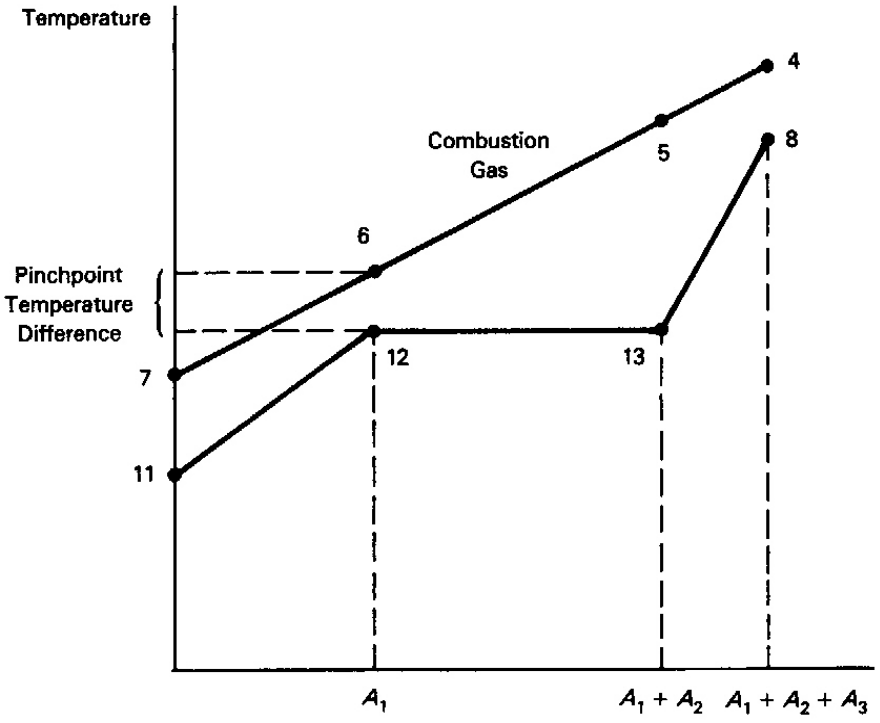


**FIGURE 9.6** Diagram of HRSG temperature–steam enthalpy differences.

other cycles in the family. Take the HRSG gas exit temperature as 350°F to avoid condensation.

Solution

The spreadsheet in Table 9.1 follows the notation of Figures 9.5 and 9.6. It tabulates three combined-cycle cases in which the boiling temperatures, $T_{12} = T_{13}$, were selected as 300°, 400°, and 500°F. These temperatures, together with the throttle and condensing temperatures and the turbine efficiency, determine the Rankine-cycle thermodynamic conditions (neglecting pump work). Equation (9.5) relates the HRSG enthalpy changes to the corresponding gas temperatures. Thus with a mass ratio $R_{\text{mass}}$ given by $(h_8 - h_{11})/(T_4 - T_7)$, the pinchpoint temperature $T_6$ for Case 2 is

$$T_6 = T_7 + (m_s/m_g C_{pg})(h_{12} - h_{11}) = T_7 + (h_{12} - h_{11})/R_{\text{mass}}$$

$$= 350 + (375.1 - 68)/2.82 = 350 + 108.9 = 459°\text{F}$$

**TABLE 9.1** Spreadsheet Solution to Example 9.1

| Combined cycle - Refer to fig. 9-5 and 9-6 for notation | | | | |
|---|---|---|---|---|
| | case 1 | case 2 | case 3 | |
| T7,F | 350 | 350 | 350 | HRSG exit temp., F |
| T4,F | 813 | 813 | 813 | gas turbine exit temp.,F |
| T11,F | 100 | 100 | 100 | feedwater in temp.,F |
| T12,F | 300 | 400 | 500 | boiling temp.,F |
| T12=T13,F | 300 | 400 | 500 | boiling temp.,F |
| T8,F | 700 | 700 | 700 | throttle temp.,F |
| p8=p12 | 67 | 247.26 | 680.86 | throttle pressure, psia |
| h11,Btu/lb | 68 | 68 | 68 | feedwater in enthalpy |
| h12,Btu/lb | 268.7 | 375.1 | 487.9 | sat liq enthalpy |
| h13,Btu/lb | 1179.7 | 1201 | 1202.2 | sat vapor enthalpy |
| h8,Btu/lb | 1381.2 | 1371.7 | 1347 | throttle enthalpy |
| h12-h11 | 200.7 | 307.1 | 419.9 | Q in economizer |
| h13-h12 | 911 | 825.9 | 714.3 | Q in boiler |
| h8-h13 | 201.5 | 170.7 | 144.8 | Q in superheater |
| h8-h11 | 1313.2 | 1303.7 | 1279 | Q in HRSG |
| T4-T7,F | 463 | 463 | 463 | HRSG temp. drop, F |
| Rmass | 2.84 | 2.82 | 2.76 | mgCpg/ms, Btu/lb-R |
| T6,F | 420.76 | 459.06 | 502.00 | gas temp at pinch,F |
| del Tpp,F | 120.76 | 59.06 | 2.00 | pinchpoint temp. diff.,F |
| Q,Btu/lbg | 127.05 | 127.05 | 127.05 | HRSG heat transfer,Btu/lbg |
| S8,Btu/lb-R | 1.849 | 1.7 | 1.571 | throttle entropy, Btu/lb-R |
| h9s,Btu/lb | 1032 | 949 | 876 | isentropic exit enthalpy |
| Wts,Btu/lb | 349.2 | 422.7 | 471 | isentropic turbine work |
| eff. turb | 0.88 | 0.88 | 0.88 | steam turbine efficiency |
| Wst,Btu/lbs | 307.30 | 371.98 | 414.48 | st. turb. work,Btu/lbsteam |
| eff. Rank | 0.23 | 0.29 | 0.32 | Rankine cycle efficiency |
| Qc,Btu/lbg | 256.78 | 256.78 | 256.78 | combustor heat transfer |
| Wgt,Btu/lbg | 64.02 | 64.02 | 64.02 | gas turbine work |
| eff. G.T. | 0.25 | 0.25 | 0.25 | gas turb. efficiency |
| Wtot,Btu/lbg | 93.75 | 100.27 | 105.19 | Wtot = Wgt+ Wst(ms/mg) |
| eff,cc | 0.37 | 0.39 | 0.41 | Combined cycle eff. |
| T7,F | 350 | 350 | 350 | |
| T6,F | 421 | 459 | 502 | |
| T5,F | 742 | 752 | 761 | |
| T4,F | 813 | 813 | 813 | |

and the pinchpoint temperature difference is

$$T_6 - T_{12} = 459 - 400 = 59°\text{F}$$

Again, by Equation (9.5),

$$T_5 = 350 + (1201 - 68)/2.82 = 350 + 401.8 = 752°\text{F}$$

With temperatures and enthalpies determined, work, heat, and efficiency values may be determined as usual, observing carefully the distinction between steam-mass and gas-mass references. It is seen that Case 2 has a satisfactory pinchpoint temperature difference and a combined-cycle efficiency of 39%, which is significantly greater than that of the gas turbine cycle (25%) and Rankine-cycle (29%) operating separately. The temperature distributions for this case are shown in Figure 9.7.

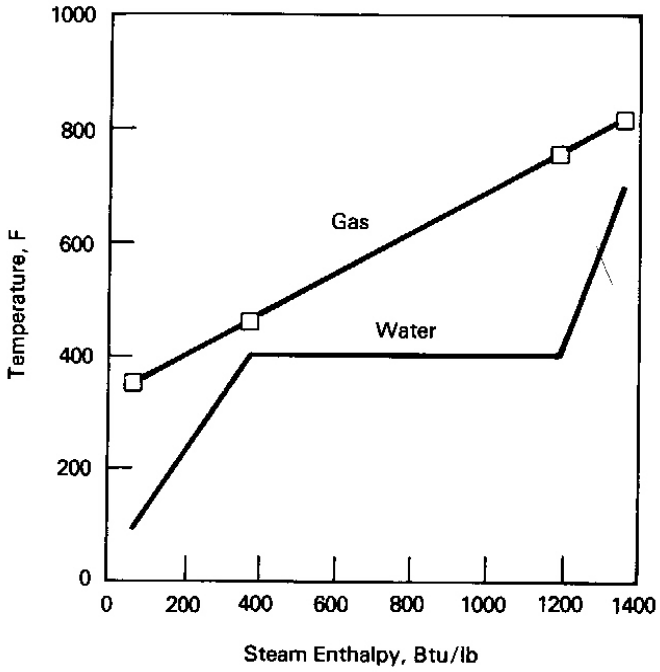


**FIGURE 9.7** Temperature distributions for the heat-recovery steam generator of Example 9.1 (Case 2).

More than one gas turbine could be used in conjunction with a single steam turbine by using a larger HRSG and multiple gas turbine exhaust ducts. Alternatively, each gas turbine may have its own HRSG, with all HRSGs thermally coupled to the steam turbine through feedwater and steam line headers.

An HRSG may be designed to burn additional fuel at its inlet using oxygen remaining in the gas turbine combustion gas to raise the temperature the HRSG gas and provide higher heat transfer to the water. Such a design is called a *fired HRSG*, and its use is usually referred to as *supplemental firing*.

Figure 9.8 shows large heat-recovery steam generators built for a nominal 450-MW combined-cycle plant in Texas utilizing three 100-MW gas turbines and one 140-MW steam turbine.

The Comanche power station, located near Lawton, Oklahoma, is an example of a combined-cycle facility that employs HRSGs. Two Westinghouse simple-cycle natural-gas-fired gas turbines, as diagramed in Figure 9.9, drive 85-MW electrical generators and exhaust into separate HRSGs designed for supplemental firing. Steam at 1200 psia and 950°F produced by the HRSGs is supplied to one nonreheat, single-extraction (not shown) steam turbine that drives a 120-MW electrical generator.

The Comanche unit, first operated in 1974 (ref. 10) was upgraded in 1986 (ref. 11), resulting in a measured plant heat rate of 8508 Btu/kW-hr (40.1% thermal efficiency), with a gas turbine inlet temperature of 1993°F, an HRSG gas inlet

**FIGURE 9.8** Heat-recovery steam generators for a cogeneration facility at Texas City, Tex., operated by Enron Power Corp., a subsidiary of Enron Corp.

temperature of 1200°F, and supplemental firing. In 1986, the plan was indentified by the Utility Data Institute as the most efficient steam-electric generating station in the United States, with an average net plant heat rate of 8821 Btu/kW-hr (thermal efficiency of 38.7%).

High-temperature combined-cycle plants are now achieving thermal efficiencies exceeeding 50%. A combined-cycle heat rate for a United Technologies Turbo Power FT8 gas turbine is said to operate at a gross plant heat rate of 6815 Btu/kW-hr (50.1%) based on lower heating value (ref. 51). Reference 50 indicates that the Pegus Unit 12 combined-cycle cogeneration plant in the Netherlands produces 223.3 MW at maximum electrical output, with a net electrical yield of 51.74% based on lower heating value. According to reference 67, "Both GE and Siemens Westinghouse turbines will be able to break the 60 per cent efficiency barrier in combined-cycle operation, and a 3 to 6 per cent reduction in $CO_2$ emissions should be possible because of the increased efficiency."

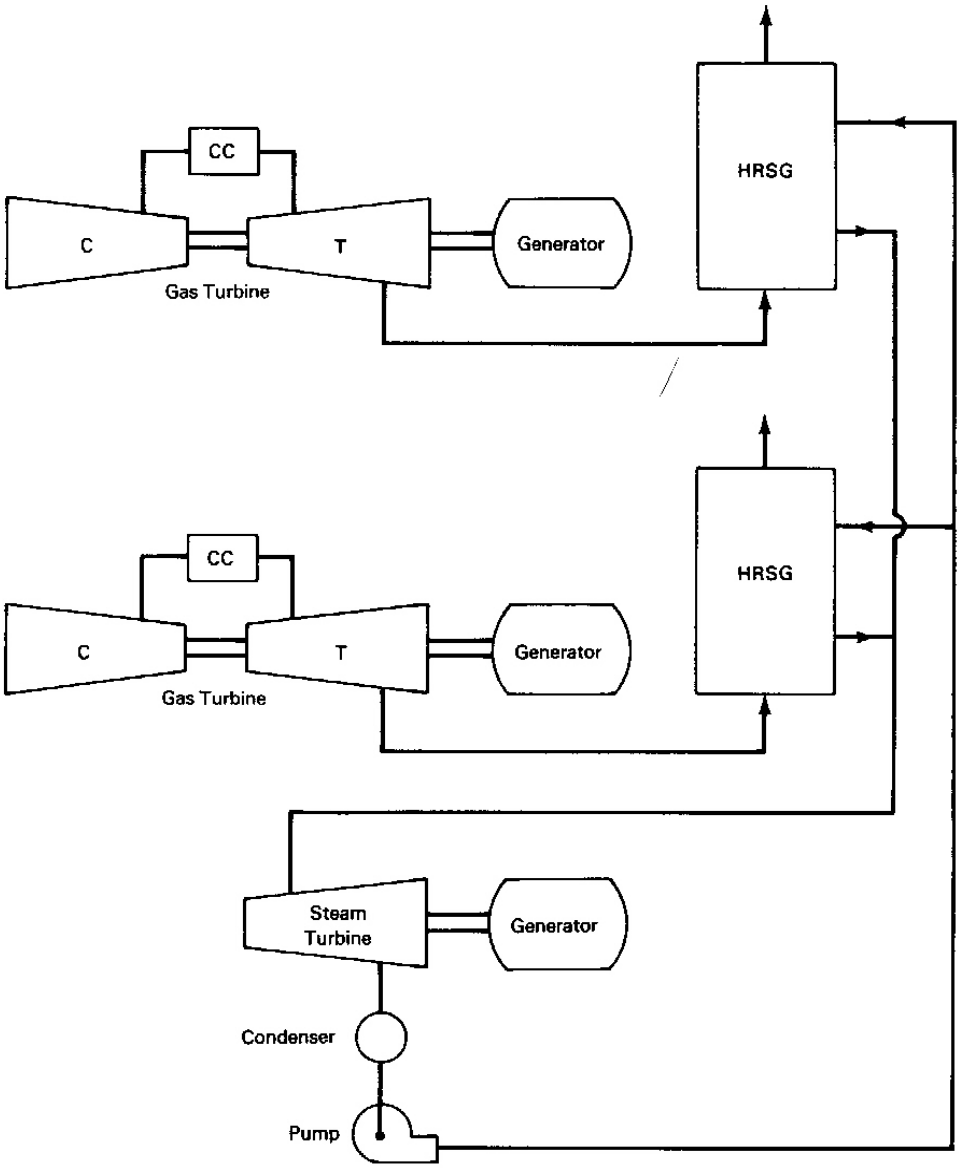


**FIGURE 9.9** Schematic of Comanche Station combined-cycle plant.

## 9.3 Integrated Gasification Combined-Cycle (IGCC) Power Plants

### The Cool Water IGCC Plant

One approach to the problem of clean coal utilization lies in the technology exemplified by the Cool Water integrated gasification combined cycle (IGCC) power plant located near Barstow, California. This plant, which went into operation in 1984, demonstrated the capability of producing power for the

**FIGURE 9.10** Cool Water integrated gasification combined-cycle plant near Daggett, Calif. (Courtesy of Cool Water Coal Gasification Program.)

Southern California Edison System with very low levels of pollutants by using both low-sulfur and medium-sulfur coals. The Cool Water demonstration plant shown in Figure 9.10 (named after the ranch on which it is located) utilized a coal gasification technique known as the Texaco process. The medium-heating-value synthetic gas called *syngas* produced by the process has about one-third the heating value of natural gas, about 265 Btu per standard cubic foot on a dry basis.

As it is produced, the syngas is first cooled, then treated to remove pollutants, and finally burned to drive turbine generators, as seen in Figure 9.11. The initial cooling in the syngas coolers produces saturated steam,which is later superheated by gas turbine exhaust gas in an HRSG, to power a steam turbine (path A in the diagram). The syngas emerging from the coolers (path B) is processed to remove particulates and sulfur and to control oxides of nitrogen, and is then burned in the gas turbine to produce additional power. The high-temperature gas turbine exhaust (path C) then passes through the heat-recovery steam generator, adding energy to the steam before it passes to the steam turbine. Thus the gasifier flows and the steam turbine and gas turbine flows interact, hence the name "integrated gasification combined cycle," IGCC.

The Texaco process requires oxygen of at least 95% purity to gasify the coal in the gasifier. The Cool Water plant thus has a small, independently owned oxygen plant (seen surrounding the single tower left of center in figure 9.10) that separates

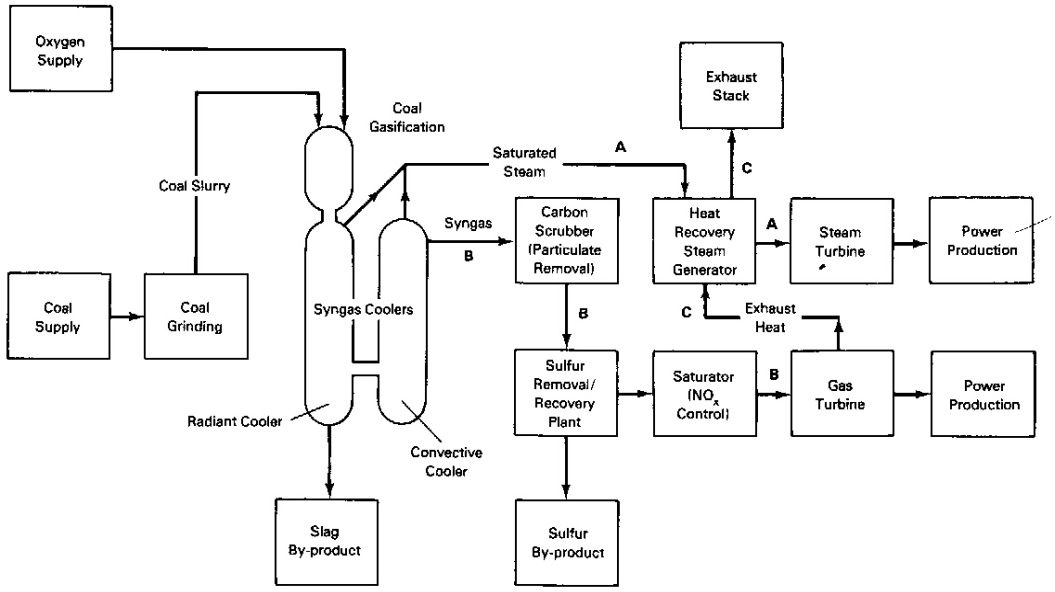


**FIGURE 9.11** Cool Water coal gasification program full heat-recovery system. (Courtesy of Cool Water Coal Gasification Program.)

oxygen from air to feed the gasifier. The Cool Water plant produces oxygen of 99.5% purity in order to produce argon as a by-product (as mentioned earlier, the process otherwise requires only 95% purity). Nitrogen is also a by-product. Oxygen is produced continually for gasifier use, but oxygen is also stored so that the IGCC plant can continue to operate if the oxygen plant is shut down.

A coal slurry, a mixture of nominally 60% coal and 40% water produced in a wet grinding process, is introduced with oxygen into the Texaco gasifier (Figure 9.11), where partial combustion of the coal takes place at about 600 psig and 2500°F. The gasifier yields a mixture of mainly carbon dioxide, carbon monoxide, and hydrogen gases, with sulfur primarily in the form of hydrogen sulfide. A relatively inert slag containing most of the mineral matter of the coal passes from the gasifier into a pool of water in the bottom of the radiant cooler. The slag is taken out periodically through a lockhopper process. The seal at the bottom of the radiant cooler is maintained by the water that is recycled.

The syngas, after cooling in the radiant and convective coolers, passes through a carbon scrubber, where a water spray removes most of the particulates and further cools the gas. After additional cooling to ambient temperature, the gas flows to a sulfur-removal unit, where a solvent removes the hydrogen sulfide and therefore most of the sulfur from the stream. The relatively particle-free and sulfur-free gas is then saturated with moisture to control the formation of oxides of nitrogen ($NO_x$) during combustion in the gas turbine. The water-quenching process suppresses $NO_x$ formation by reducing the gas combustion temperature, and it also increases the turbine power output by adding to the mass flow in the gas turbine combustor. Combustion gases from the gas turbine then pass through the heat

recovery steam generator, where they produce additional steam as they drop in temperature to about 400°F. The combustion products leaving the plant are remarkably pollutant free. Performance of the Cool Water Station is summarized in Table 9.2 below.

**Table 9.2 Cool Water IGCC Station Nominal Performance**

| | |
|---|---|
| Gas turbine electric generator power | 65 MW |
| Steam turbine electric generator power | +55 MW |
| **Gross power** | 120 MW |
| Air-separation oxygen plant | –17 MW |
| Internal plant consumption | – 7 MW |
| **Net power** | 96 MW |
| Design heat rate | 11,510 Btu/kW-hr |
| Observed heat rate | 10,950 Btu/kW-hr |

*Source*: Reference 3.

The operators of the Cool Water station have demonstrated values of critical pollutants well below current environmental limits for both permit and regulatory limits and New Source Performance Standards (NSPS), as indicated in Table 9.3. The Cool Water plant has operated successfully with Utah run-of-mine coal with 0.4% sulfur, Illinois #6 coal with 3.1% sulfur, and Pittsburg #8 coal with 2.9% sulfur. The sulfur removal process in the plant yields about 99.6% pure elemental sulfur, which can be sold for the production of sulfuric acid and fertilizers. The slag produced by the gasifier is considered nonhazardous and suitable for the production of road-making materials or cement.

**Table 9.3 Emissions from the Cool Water Station HRSG (lb/million Btu)**

| | High Sulfur Coal $SO_2$ | Low Sulfur Coal $SO_2$ | $NO_x$ | CO | Particulate Matter |
|---|---|---|---|---|---|
| Permit and regulatory limit | 0.16 | 0.033 | 0.13 | 0.07 | 0.01 |
| Utah coal | – | 0.018 | 0.07 | 0.004 | 0.001 |
| Illinois #6 | 0.068 | – | 0.094 | 0.004 | 0.009 |
| Pittsburgh #8 | 0.122 | – | 0.066 | <0.002 | 0.009 |
| Federal NSPS | 0.6 | 0.24 | 0.6 | – | 0.03 |

*Source*: Reference 3

The net effect of the plant then is to generate power efficiently by utilizing widely available coals with sulfur content up to 3.5% in an environmentally sound

way while producing nonhazardous waste that offers the possibility of constructive use.

It should be understood that the Cool Water plant was built as a demonstration plant to prove a technology on a large but not a full scale. Engineering studies based on the Cool Water operating experience (ref. 4) have indicated that a 360-MW full-scale IGCC plant using Illinois #6 coal could be built with a net heat rate of 9000 Btu/kW-hr at a capital cost of $1530/kW and with operating and maintenance costs of 2.3 cents/kW-hr (or 5.2 cents/kW-hr, which includes all fixed charges) (ref. 3). These costs are competitive with those for conventional new coal-burning power plants using flue gas desulfurization.

An important feature of the IGCC plant concept is the attractiveness of *phased construction*. A conventional coal-burning steam power plant must be constructed as a unit and takes a relatively long time to erect. On the other hand, one or more gas turbines of a planned IGCC plant may be quickly put into service using natural gas as a fuel. Additional gas and steam turbines may be added later to transform the plant into a combined-cycle plant, with coal gasifiers and an oxygen plant added still later at a third stage. Because the units may be paid for as they are built, phased construction offers significant financial benefits as well as ordely growth.

Significant materials problems have been overcome in the Texaco and Cool Water plant technology. The inside of the gasifier requires refractory materials to withstand the severely corrosive high-temperature environment. Cool Water experience (ref . 5) indicates that 10,000–14,000 hours of refractory life is attainable. This implies that gasifier overhaul will be required at least every two years. Additional problems with cooler tube-wall materials, coal slurry pumps, and piping; and other severe material operating environments offer challenges for materials research to improve IGCC operation.

Several of the references expand on the idea of cogeneration–*polygeneration*– by pointing out that, based on the Cool Water technology today, a single facility whose only major requirements are air, water, and coal can simultaneously produce electricity, steam, sulfur, inert slag for road construction, oxygen, nitrogen, hydrogen, carbon monoxide, carbon dioxide, argon, methanol, other chemical products, and even syngas.

**The Dow Gasification Process**

Another coal gasification process combined-cycle system (CGCC), developed by Dow Chemical Co., operates in Plaquemine, Louisiana. Like the IGCC system, the Dow process reacts a coal slurry with oxygen to produce syngas, from which most of the sulfur is removed for by-product use. The raw syngas from the gasifier produces steam in an HRSG, is cooled, passes through pollutant removal equipment, and is burned in gas turbines. Reference 47 indicates that “of the new coal-based technologies, the CGCC system has the highest efficiency and the lowest emission of environmental pollutants.” The 161-MW plant, built in the remarkable time of twenty-one months, was completed in 1987. The reference indicates for CGCC plants a net heat rate based on lower heating value of 8670

Btu/kW-hr (39.4%) and a total capital cost of $1201/kW, based on 1988 dollars. Additional information on combined-cycle coal gasification systems is given references 58, 59, and 65. Tampa Electric's 250-MW IGCC Polk Power Station began commercial operation in 1996. A website (ref. 65) indicates that the station is 10-12% more efficient than conventional coal-fired plants.Three dimensional views may be seen at the website.

**9.4 Combustion in Fluidized Beds**

The need to develop environmentally sound methods for utilizing a variety of coals, industrial and municipal wastes, and other solids as fuels has stimulated research in a variety of areas. Another prominent and promising technology applicable to these goals is *fluidized bed combustion* (FBC). Atmospheric fluidized bed combustors (AFBCs) operate near atmospheric pressure; pressurized fluidized combustors (PFBCS) are enclosed in a pressure vessel and operate at a pressure of about 12 atmospheres.

As the name suggests, a principal unique feature of this technology is that combustion takes place in a bed of solid particles supported in vigorous, turbulent motion on an upwardly directed stream of air. The bed may consist of a combination of particles of fuel, sand, ash, waste materials, limestone, and other compounds, depending on the function and design of the fluidized bed combustor. The key point is that these materials mingle and react in continually changing orientations, providing ample opportunity for intimate contact of fuel and oxidizer and for removal of combustion products, while supported on the fluidizing air stream. The name *bubbling bed* is sometimes used to decribe this action.

It has been found that horizontal water tubes located within the fluidized bed, in crossflow to the upward air stream, experience very high heat transfer coefficients in comparison with those in normal furnace convective and radiative environments. It is even more important that fluidized beds containing coal and limestone produce combustion gases with both low sulfur content and low concentrations of oxides of nitrogen.

*Limestone* reacts with sulfur in the coal to produce particles of calcium sulfate that are removed as bed materials are renewed. More specifically, the limestone, $CaCO_3$, reacts to form $CO_2$ and lime, CaO:

$$CaCO_3 \Rightarrow CaO + CO_2$$

and the CaO reacts with the sulfate vapors:

$$H_2SO_4 + CaO \Rightarrow CaSO_4 + H_2O.$$

The calcium sulfate forms as a solid that becomes a bed material, and the water vapor passes off as a component of the flue gas.

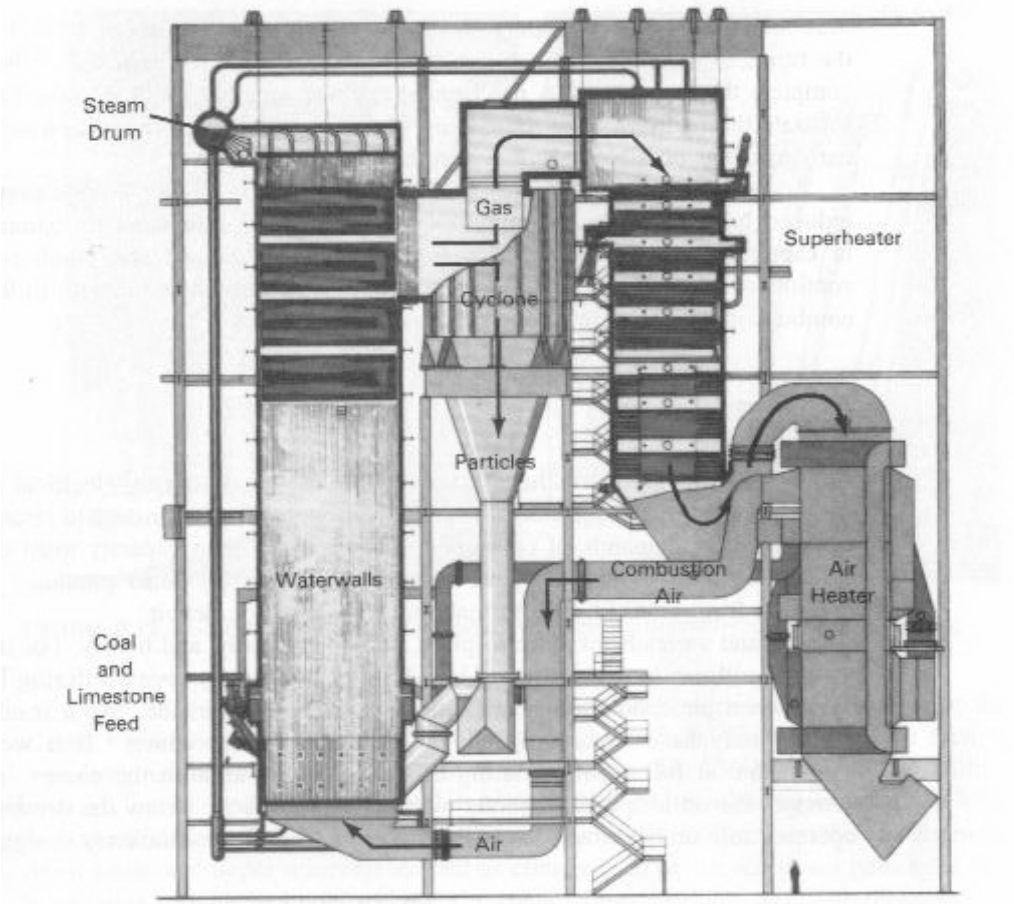


**FIGURE 9.12** Circulating fluidized bed power plant in Nucla, Colo. (Courtesy of Pyropower Corp.)

Oxides of nitrogen ($NO_x$) produced by the FBC are maintained at low values, because bed and gas temperatures are well below those at which $NO_x$ forms in conventional combustors. The bed temperature is determined primarily by the rates of air and fuel supplied. Normally, FBC bed temperatures are about 1550°F, compared with conventional furnace temperatures in the neighborhood of 3000°F. The reactivity of nitrogen is low at 1500°F, and chemical equilibrium calculations and laboratory observations show that the nitrogen in flue gas is almost entirely in its normal, diatomic form.

The combustion of coal or other solids occurs largely at the interface between the solid and the surrounding oxidizing gases. The rate at which the solid burns depends on the rate at which oxygen is brought to the solid interface and on the rate at which combustion products are removed, as well as on the rate of chemical reaction at the interface itself. The vigorous relative motion of the bed particles and the intervening air flow provide an excellent mechanism for delivery of oxygen to and the transport of combustion products from the interface.

Normally, FBC occurs with enough excess air, in the primary supporting air

stream and possibly in a secondary over-fire air flow, that combustion is virtually complete. Flyash and other airborne particles are removed by centrifugal separators and baghouse filters. Solids from the separators may be reinjected into the bed to further ensure almost complete burnup of carbon.

The *circulating fluidized bed* (CFB) combustor (refs. 26 and 30) is one in which smaller solid bed materials are carried upward by the combustion air/gas stream. A return passage transports the unburnt and inert particles and part of the combustion gas back to the main furnace, allowing the remaining flue gas to pass to the heat-recovery area, as seen in Figure 9.12. The solid bed materials continue to burn as they circulate, thus maintaining an approximately uniform temperature of about 1550°F throughout the furnace. As a result, there is a long residence time for particles of the furnace to complete their reactions. A mechanical cyclone separator built into the furnace helps to separate the particles from the exiting flue gas. As a result, reinjection of the unburnt carbon makes possible very high combustion efficiencies.

According to reference 26, CFB designs achieve higher combustion efficiency, reduced $NO_x$ emissions, minimum CO formation, and reduced limestone utilization in capturing $SO_2$ when compared with bubbling fluidized bed combustors. Much continues to be learned about problems and opportunities inherent in fluidized bed combustion as more units come into use. In a December 1998 work (ref. 65), the U.S. Department of Energy (DOE) proposed a 379-MWe, pressurized circulating fluidized bed combustor combined-cycle plant with a net efficiency of 47%.

## 9.5 Energy Storage

It has been observed that there is no existing means of storing electrical power on a large scale. As a consequence, power generation varies from instant to instant, to satisfy the immediate demands of consumers. Utility generation capacity must therefore be great enough to satisfy the peak demand, or the utility must purchase power at a premium from other utilities to make up its generation deficit.

Demand varies from place to place, seasonally, daily, and hourly. For instance, the loads of utilities in the southern United States are usually greatest during hot summer days, when air conditioning and industrial demands coincide. As a result, southern utilities may have excess capacity at night and in the winter. It were possible to generate a full capacity during off-peak hours and store the energy in excess of demand, the utilities could operate with installed capacity below the demand peak and operate more units as base-load plants close to their high-efficiency design points.

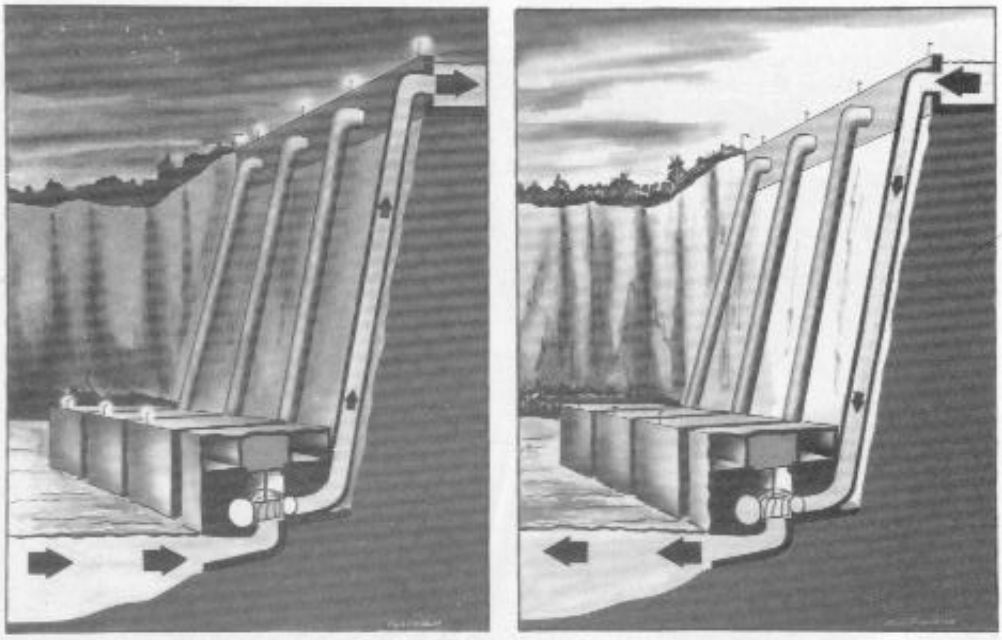

**FIGURE 9.13** Schematic of pumped storage. (Courtesy of Benham-Holway Power Group.)

**Pumped Storage**

One approach to off-peak energy storage utilizes a high reservoir into which water from a low elevation is pumped, using electricity generated during off-peak hours. Thus energy may be stored in the form of potential energy of the elevated water for later use during peak loads. There are about thirty such *pumped-storage* facilities in the United States.

Figure 9.13 depicts the two phases of operation of a pumped-storage facility. These installations usually employ motor-generator sets driven by hydraulic turbines. *Mechanically reversible pump-turbines* generate electricity by using water from an elevated reservoir during periods of peak demand. When there is an excess of base-load power, the motor-generators can be reversed to drive the pump-turbines as pumps for filling the reservoir.

It is clear that net energy is lost in the use of pumped storage. Its success relies on the availability of cheap power during off-peak hours and consistent demand for electricity, with its associated high price during peak hours. Pumped storage allows utilities to generate more electricity with their most efficient base-load plants instead of handling peaks with less efficient equipment.

Figure 9.14 is a photograph of the Salina pumped-storage facility (ref. 34) of the Grand River Dam Authority, located about 50 miles from Tulsa, Oklahoma. The facility was designed for gradual expansion, in three steps, from the 130-MW configuration that went online in 1968, to the current 260-MW facility shown in

**FIGURE 9.14** Salina pumped-storage facility. (Courtesy of Benham-Holway Power Group.)

the figure, to a 520-MW final modification. The eventual completion of the project will require the development of an additional upper reservoir as well as construction of six additional penstocks and the installation of their hydroelectric pump-turbine motor-generator sets. The present plant is capable of producing power at full-rated load for eight hours a day or at part load for twelve hours a day. The reservoir is 251 feet above the lower lake. The penstocks are 14 feet in diameter and 720 feet long.

Reference 36 identifies an early pumped-storage facility named Rocky River at New Milford, Conn., which was in operation in 1928. The limited number of high head surface sites for such facilities, the high capital cost of building a dam, and the large land area impacted by these facilities make the future use of pumped storage questionable. Reference 37, however, predicted continued growth in pumped storage capacity. One possibility that would support such growth is to have the upper pool at ground level and to use underground mines for the lower pool (ref. 38). Another is the development of low head facilities.

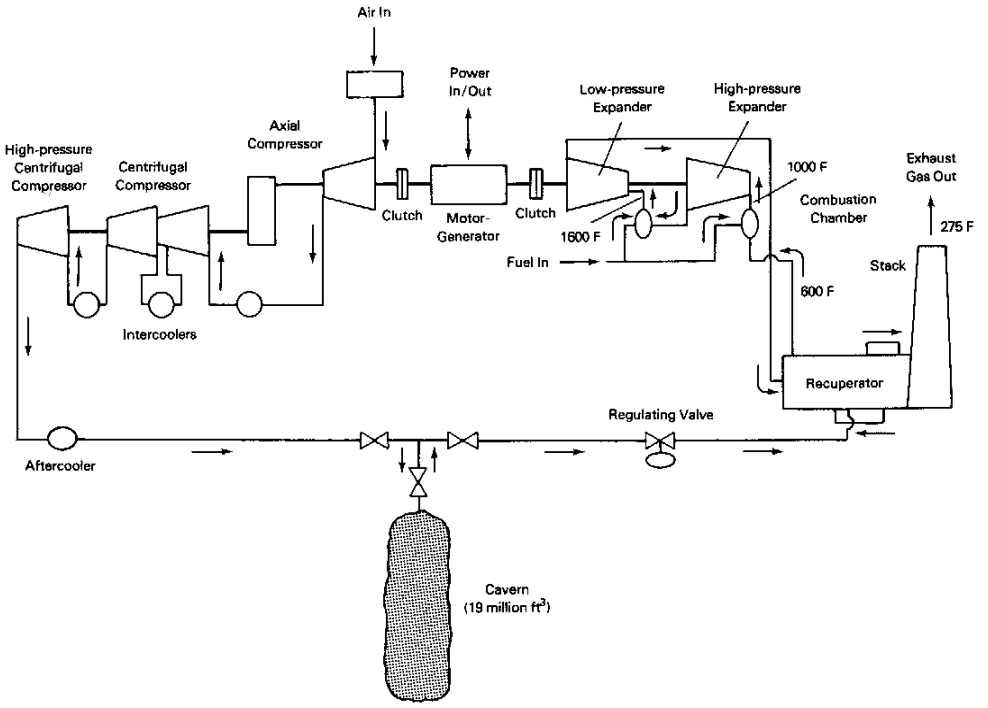


**FIGURE 9.15** Schematic of the Alabama Electric Cooperative compressed-air energy-storage plant. (Courtesy of the *EPRI Journal.*)

## Compressed-Air Energy Storage

A relatively new approach to energy storage is *compressed-air energy storage* (CAES), which employs underground caverns for storage of air under pressure (refs. 25 and 49). Air is compressed into the cavern using off-peak power and later is released to oxidize fuel in a gas turbine combustor to generate electrical power during hours of peak demand. The first CAES plant, a 290-MW unit, first operated at Huntorf, West Germany, in 1978. A second CAES plant located in McIntosh, Ala, with phased construction of two 110-MW units, first went on-line in May, 1991 (ref. 64).

CAES plants are located in the vicinity of underground caverns. The caverns may be natural or may be created and/or enlarged by solution-mining of underground salt domes. In solution-mining, water is pumped into a salt formation, the water dissolves salt locally, enlarging the cavern, and the resulting brine is pumped to the surface, where the salt is driven from the solution and the water reused.

Figure 9.15 shows a schematic of the McIntosh plant. During off-peak hours a motor-generator, powered by electricity produced elsewhere in the utility system and with turbine-expander clutch disengaged, drives the compressor set that packs air into the salt cavern. Later, air is allowed to escape from the cavern to oxidize fuel at the high cavern pressure, forming combustion gas to pass through the gas turbines (expanders) that drive the motor-generator in the generation mode with

the compressor clutch disengaged. The generator thus is able to return electricity to the utility system during periods of peak demand.

The CAES plant is essentially a gas turbine in which the compression process is decoupled from the power delivery process. During daily cyclical operation, the mass of air supplied to the cavern at night is utilized during the day. Since the charging period may be different than the utilization period, the average mass rates of storage and delivery may differ. The McIntosh plant is designed for twenty-six hours of storage capacity and therefore does not operate on a strict daily cycle but rather on a weekly cycle that takes advantage of less expensive weekend power.

The presence of the recuperator in the McIntosh plant, the first in use in a CAES facility, provides regeneration, which, as discussed in Chapter 5, substantially reduces gas turbine fuel consumption and thus improves plant efficiency. Regeneration may also be accomplished by absorption and storage of the heat of compression of the air in an aftercooling, high heat capacity heat exchanger such as a pebble bed recuperator. The stored energy is later returned to the air discharged from the cavern as it flows to the turbines.

The success of a CAES plant, like that of pumped storage, depends on the availability of cheap, off-peak power. The objective is to drive the compressor train during these periods so that high-priced power may be produced later in periods of high demand. It should be noted that the compression process is not only decoupled mechanically from the power delivery process, but the compression process may take place over a longer period of time than the period of CAES power production. This allows the use of smaller compressors than would be needed for a conventional peaking gas turbine. According to reference 25, the Huntorf plant compresses for 4 hours, and the McIntosh plant for 1.7 hours, for each hour of power production. CAES may become a more viable option in the United States than surface pumped storage because of the existence of more potential sites and lower land surface area requirements for CAES.

## 9.6 District Heating and Cooling and Cogeneration

Comfort heating and cooling in homes, businesses, and industry consumes large quantities of energy. Much of this low-temperature-energy use is accomplished by the direct or indirect burning of fossil fuels and high temperature. Electrical resistance heating, especially, and heat pumps may be included in this because the electricity they consume is produced largely from high-temperature sources. Many believe that these are inappropriate uses of fossil fuels, in a conservation sense, because of the unnecessary loss of the availability of high-temperature energy to do work. It is simply a reflection of the desirability of using high temperatures where needed and low-temperature sources for low-temperature functions. For instance, it is no revelation that some of the obligatory heat rejection by modern heat engines is at a high enough temperature to supply energy for comfort heating and cooling.

*District heating*, the provision of heat to a populated area by a nearby central heating plant, has been in use for one hundred years or more. More recently the addition of cooling to such plants has become widespread. Now, colleges and universities frequently have such a facility. Shopping malls and blocks of business districts in many cities also take advantage of the economic benefits provided by a central plant. This is usually accomplished through the use of boilers that produce hot water or steam for heating, and by vapor compression or steam-driven absorption refrigeration machines that produce chilled water for cooling. Water, steam, or brine is usually used to deliver the energy to the user.

In municipal facilities, the steam, water, or brine is metered and circulated in insulated pipes under the streets to air-handling units and other point-of-use devices in the customers' buildings, and thence to return pipes that bring the fluid back to the central plant or, in single-pipe one-way systems, to sewer mains.

Until recently, most of the district heating facilities the United States did not find significant advantage in producing electrical power and using the waste heat for district heating, cooling, or industrial process energy. With Europe's more limited energy resources, *combined heat and power* (CHP), or *cogeneration*, the synergistic generation of electric power and heat, found more extensive use there than in United States following the Second World War. In fact, a number of steam turbines and closed-cycle gas turbines burning a variety fuels were developed for simultaneous electric power generation and district heating or industrial cogeneration purposes (refs. 12 and 15–20). These activities are closely related to *total energy systems*, which seek to utilize natural gas for other purposes while generating electricity (ref. 17). In the United States this term has been used in the past for the promotion of natural-gas-burning systems that provided heating, cooling, and electricity for shopping malls, colleges, and similar customers.

Some of the possible cogeneration steams include:

1. Steam turbine power with condenser heat rejection for low-temperature processes, facility heating, or district heating.

2. Steam turbine power with steam extraction or use of a back-pressure turbine for process or district heating use.

3. Steam turbine power with exhaust steam or steam extraction heat transfer to absorption refrigeration system generators for chilling processes or district cooling in summer.

4. Closed-cycle gas turbine power with coolers (intercoolers and pre-coolers) used for district heating.

5. Closed-cycle gas turbine power with coolers used with absorption refrigeration system for chilling processes or district cooling in summer.

6. Open-cycle gas turbine power with exhaust heat recovery for process use or district heating.

7. Diesel or gas reciprocating engine power with water-jacket cooling, oil cooler, and/or exhaust gas heat recovery used for process or district heating.

A measure of the efficiency of energy utilization in a cogeneration plant is the *energy utilization factor*, EUF, which is the sum of the net work, $w$, and the useful heat produced, $q_u$, divided by the energy supplied to achieve the combined heat and work, $q_{in}$, (ref. 18):

$$\text{EUF} = (w + q_u)/q_{in} \qquad [\text{dl}] \qquad (9.6)$$

Care should be taken when considering the EUF and the thermal efficiency of a plant. The EUF is not restricted by the Carnot efficiency and can therefore approach 100%. For instance, when there is no useful heat transfer, the EUF is the plant thermal efficiency. At the other extreme, when no power is produced the plant can utilize almost all the energy supplied by the fuel for useful heat; and therefore the EUF could approach 100%. Thus the EUF is a measure of the extent of productive use of the energy source, with no consideration for work–useful heat proportions. An EUF in excess of 80 percent is possible for a CHP plant.

Other efficiencies for CHP plants may be defined. For instance, a weighting factor might be used in the numerator of the EUF to attempt to give appropriate weight to both heat and work. For example, since conventional power plants convert heat to work with about 33% efficiency, one might define a special EUF* as $(w + 0.33q_u)/q_{in}$ for comparison with thermal efficiencies. While such factors may be useful in evaluating the design of a plant, they should be applied with care. Reference 18 discusses alternative definitions more fully.

## 9.7 Electricity Generation and Legislation

Historically, the electric power industry in the United States developed by recognizing the economic advantages of scale of large central plants that used extensive power transmission and distribution systems, following the lead of the great governmental hydroelectric power projects. They also recognized the enhanced growth potential inherent in the society's becoming "totally electric." The productive disposition of condensor rejected heat had no place as a revenue producer in this scheme, for the important reasons that it would reduce plant efficiency and power output and could not reach across the miles as power transmission lines could. Individual consumers as well as industry happily accepted this approach to the electrification of America, as electricity prices dropped decade after decade. Natural-gas and fuel oil companies were also there to satisfy the vast needs for heat.

More recently, energy-consuming industries came to recognize the possibilities of simultaneous power and heat generation to satisfy their energy requirements. At

the same time, a consciousness grew that there are limits to the world's energy resources and that a more thoughtful stewardship of them would be prudent, when it is economically attractive. However, in the early 1970s the OPEC oil embargo brought these notions into clearer focus, and federal legislation in 1978 brought cogeneration to everyone's attention with the enactment of *PURPA*, the *Public Utility Regulatory Policies Act* (ref. 14).

PURPA, a part of the National Energy Act, was intended to bring competition into the electric power generation business and to increase the national effectiveness of energy utilization by making cogeneration more economically attractive. It required that utilities purchase power from qualified cogenerators at a reasonable price, created tax incentives for developers, and established the *Federal Energy Regulatory Commission*, FERC, to regulate and administer the activity. Prospective cogenerators must apply to the FERC for certification as a *qualified facility*, QF. The FERC, however, left the deliberation of what constitutes a fair price to state public utility commissions. As a result, industrial cogeneration thrives in some states and is virtually nonexistent and others. PURPA requires utilities to buy electricity from QFs at the marginal cost of new generation, that is, the cost of electricity generated by new power plant if it were built, the so-called *avoided cost*.

The growth of cogeneration, state and national actions to change the regulatory structure of the electric utility industry, the difficulties of acquiring capital for large, long-term projects and other uncertainties are significantly changing the outlook and structure of the utility industry (ref. 21). Utilities now appear to be looking toward incremental and modular growth and the avoidance of long-term commitment, which is reflected in their reluctance or inability to undertake the construction of large, capital-intensive base-load plants. Legislative changes in the 1990's and beyond are bringing substantial deregulation to the industry, open access to power transmission systems, and the introduction of *merchant plants* created to offer electricity to the highest bidder in the new free-enterprise climate (ref. 66).

## 9.8 Steam-Injected Gas Turbines

Water injection has been used for many years for brief augmentation of the thrust of jet engines. More recently, liquid water injection and steam injection have been used to control the formation of $NO_x$ in gas turbines. Injection of water or steam into the combustion chamber reduces the combustion temperature, which in turn suppresses the formation of $NO_x$ caused by high temperature. Power output is maintained or increased because the injection increases both the turbine mass flow and the energy extraction by the turbine. The latter is possible because the heat capacity of steam is almost twice that of normal combustion products. Thus the enthalpy change of steam for a given temperature drop is about double that of air or combustion gas. If water is injected as a liquid, additional energy must be extracted from the combustion gas to vaporize the water.

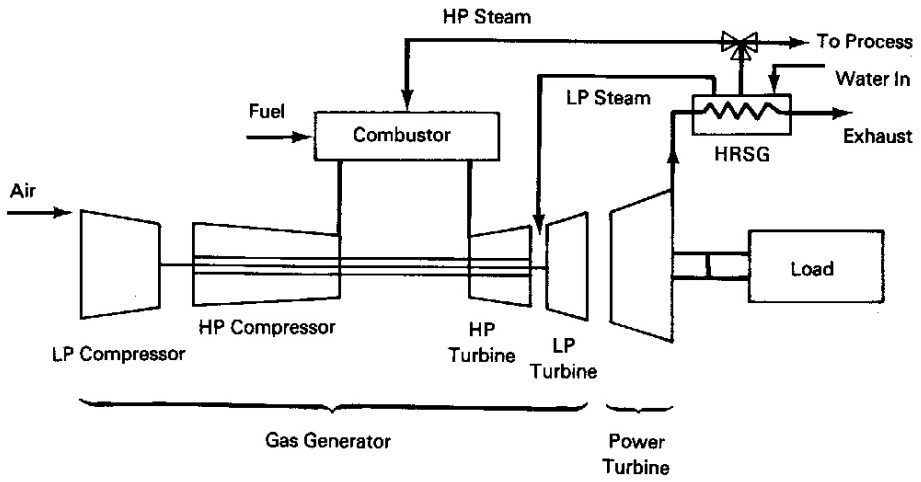


**FIGURE 9.16** Gas turbine power enhancement by steam mass injection. (Courtesy of the General Electric Co.)

As a consequence of these considerations, an important cogeneration technology is emerging. The *steam-injected gas turbine*, STIG™* or SIGT, uses the gas turbine exhaust flow through an HRSG to produce steam that is partially or entirely injected into the gas turbine combustion chamber and possibly the compressor and/or turbine, as indicated in Figure 9.16, resulting in augmented gas turbine power output. Reduced steam requirements for process use in an industrial cogeneration plant may be used to increase electrical power generation, which in turn may be sold to a local utility under PURPA if it is not needed for other on-site uses.

References 13, 22, 23, and 31 show increased power output, increased thermal efficiency, and reduced $NO_x$ as benefits of steam injection. Table 9.4, for example, lists performance measurements of the effects of steam injection into two industrial gas turbines. The table shows that as the cogeneration process steam percentage is reduced and the steam flow to the gas turbine increases accordingly, substantial increases in power output and thermal efficiency are consistently attained. Thus the steam-injected gas turbine holds considerable promise for cogeneration and process applications.

A cross-section of the General Electric LM 5000 gas turbine without steam injection is shown in Figure 9.17; a photo of the same is presented in Figure 9.18. The LM 5000 is a compact, high-performance, aeroderivative gas turbine intended for marine and industrial applications. It is derived from the CF6 family of high-bypass-ratio turbofan engines but burns either distillates or natural gas fuels. The LM 5000 has a dual-rotor gas generator and a three-stage power turbine. The manufacturer quotes a power output of 46,200 shaft horsepower (34,451 kW) and a heat rate of 9160 Btu/kW-hr at a power turbine speed of 3600 rpm for the LM 5000 without STIG.

*STIG is a trademark of General Electric Co., U.S.A.

**Table 9.4** Performance of Steam-Injected Gas Turbines with Unfired HRSG

| Cogeneration Steam Percentage | Power Output (kW) | Thermal Efficiency |
|---|---|---|
| Allison 501-KH | | |
| 100% | 3500 | 0.24 |
| 50% | 4750 | 0.30 |
| 0% | 6000 | 0.35 |
| General Electric LM5000 | | |
| 100% | 33000 | 0.33 (0.36) |
| 50% | 40000 | 0.36 (0.38) |
| 0% | 47000 | 0.38 (0.42) |

Adapted from reference 22. Data in parentheses from references 56 and 57.

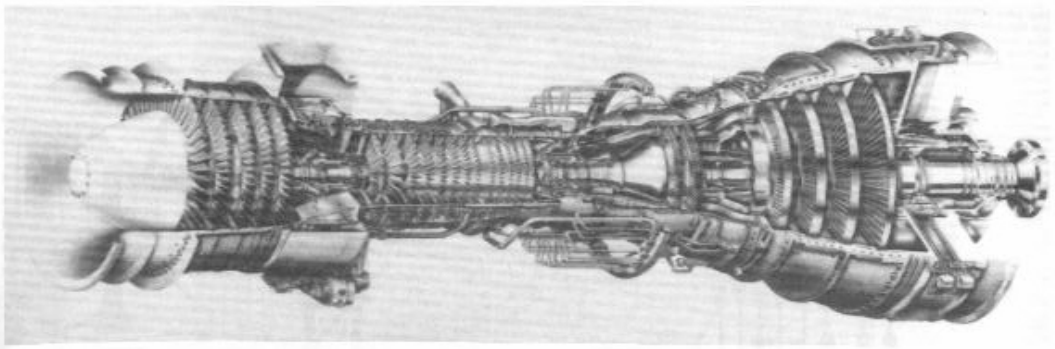

FIGURE 9.17 Cutaway of the LM 5000 (non-STIG) gas turbine, an aeroderivative of the CF6 family of turbofan engines. (Courtesy of the General Electric Co.)

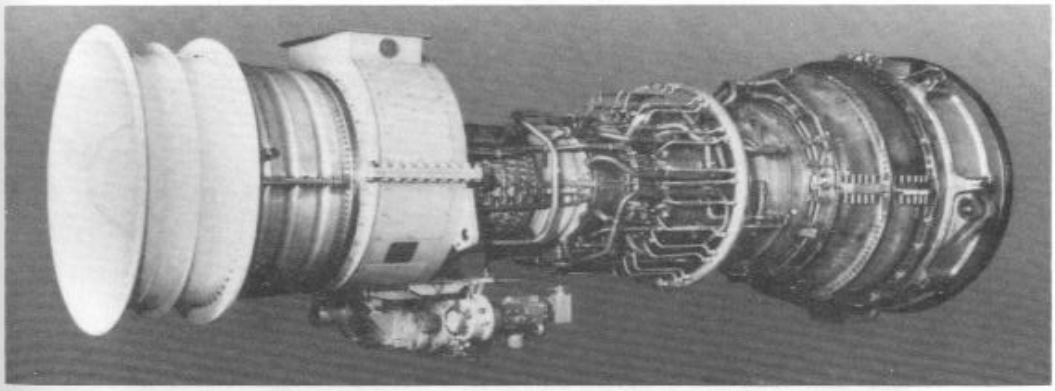

FIGURE 9.18 LM 5000 (non-STIG) engine. (Courtesy of the General Electric Co.)

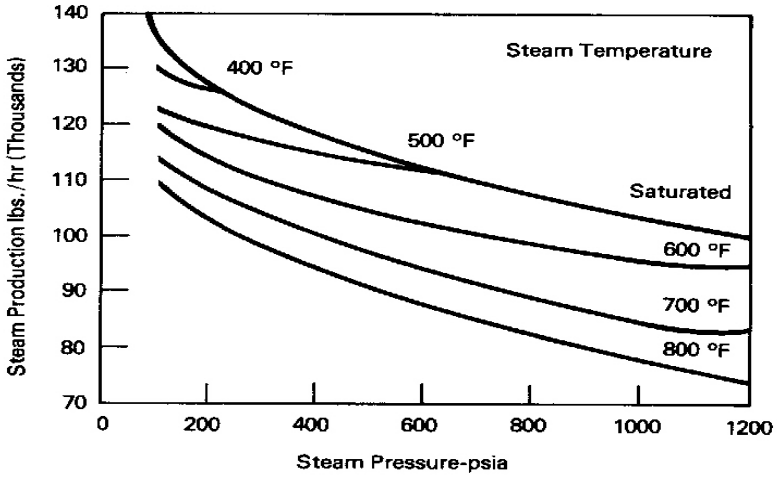


**FIGURE 9.21** Steam generation capacity of the LM 5000 gas turbine with an unfired HRSG and 30° F pinchpoint temperature difference. (Courtesy of the General Electric Co.)

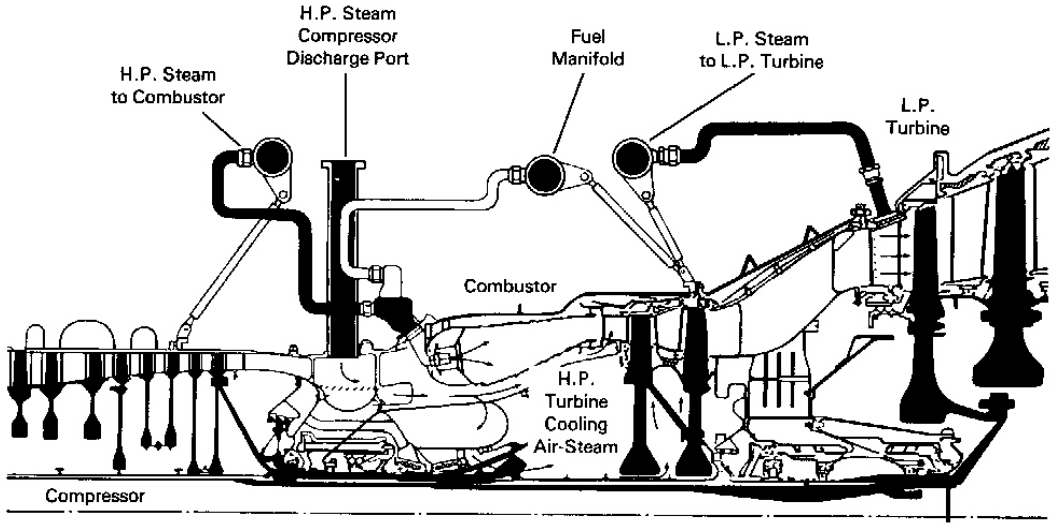


**FIGURE 9.19** Cross-section of the LM 5000 STIG engine. (Courtesy of the General Electric Co.)

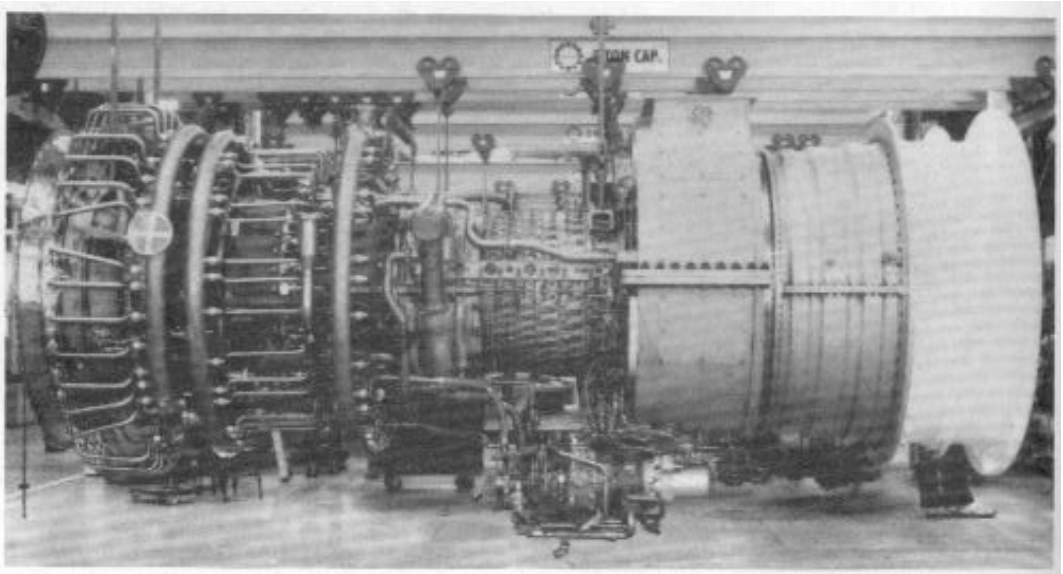

**FIGURE 9.20** LM 5000 gas generator with full STIG configuration. (Courtesy of the General Electric Co.)

A schematic of the LM 5000 STIG configuration is shown in Figure 9.19; a photo of the same is presented in Figure 9.20. The steam manifolds and injection lines may be seen in both figures. Table 9.4 shows the performance of this configuration without supplemental firing of the HRSG. With full STIG and supplemental firing, the power output increases to 72,100 shaft horsepower (53,765 kW) and a heat rate of 7580 Btu/kW-hr (or a thermal efficiency of 45%) is attained.

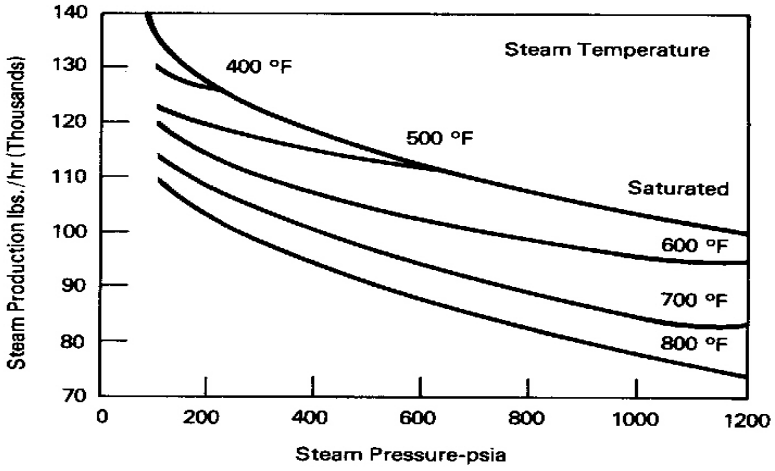


**FIGURE 9.21** Steam generation capacity of the LM 5000 gas turbine with an unfired HRSG and 30° F pinchpoint temperature difference. (Courtesy of the General Electric Co.)

Figure 9.21 shows the average steam generation capability of the engine exhaust with an unfired HRSG having a 30°F pinchpoint temperature difference. It is seen that, as expected, higher steam flow rates are obtained with reduced steam temperature and pressure for given HRSG exhaust and turbine exhaust temperatures.

A study the economic advantages of steam-injected gas turbines for utility use relative to the combined-cycle power plant (ref. 33) has shown combined cycles to be superior in unit sizes above 50 MW. However, utilities are becoming increasingly interested in plants of 50 MW or less because of their small size and quick availability.

## Intercooled Steam-Injected Gas Turbines

A modification of the steam-injected gas turbine is ISTIG, or, intercooled STIG, in which steam is injected into compressor bleed air for turbine cooling, together with steam injection into the combustor and into one or more turbine stages (ref. 22). The enhanced blade cooling allows increased turbine inlet temperature and further power and efficiency increases. The reference predicts efficiencies for ISTIG turbines better than for existing combined cycles and comparable to advanced combined cycles. Thus STIG and ISTIG show great promise for cogeneration applications and are likely to find their way into future power generation plans.

## Steam-Injected Gas Turbine Analysis

The influence of steam injection into the combustor can be analyzed with a model that accounts for the major effects on the engine performance: the added mass and

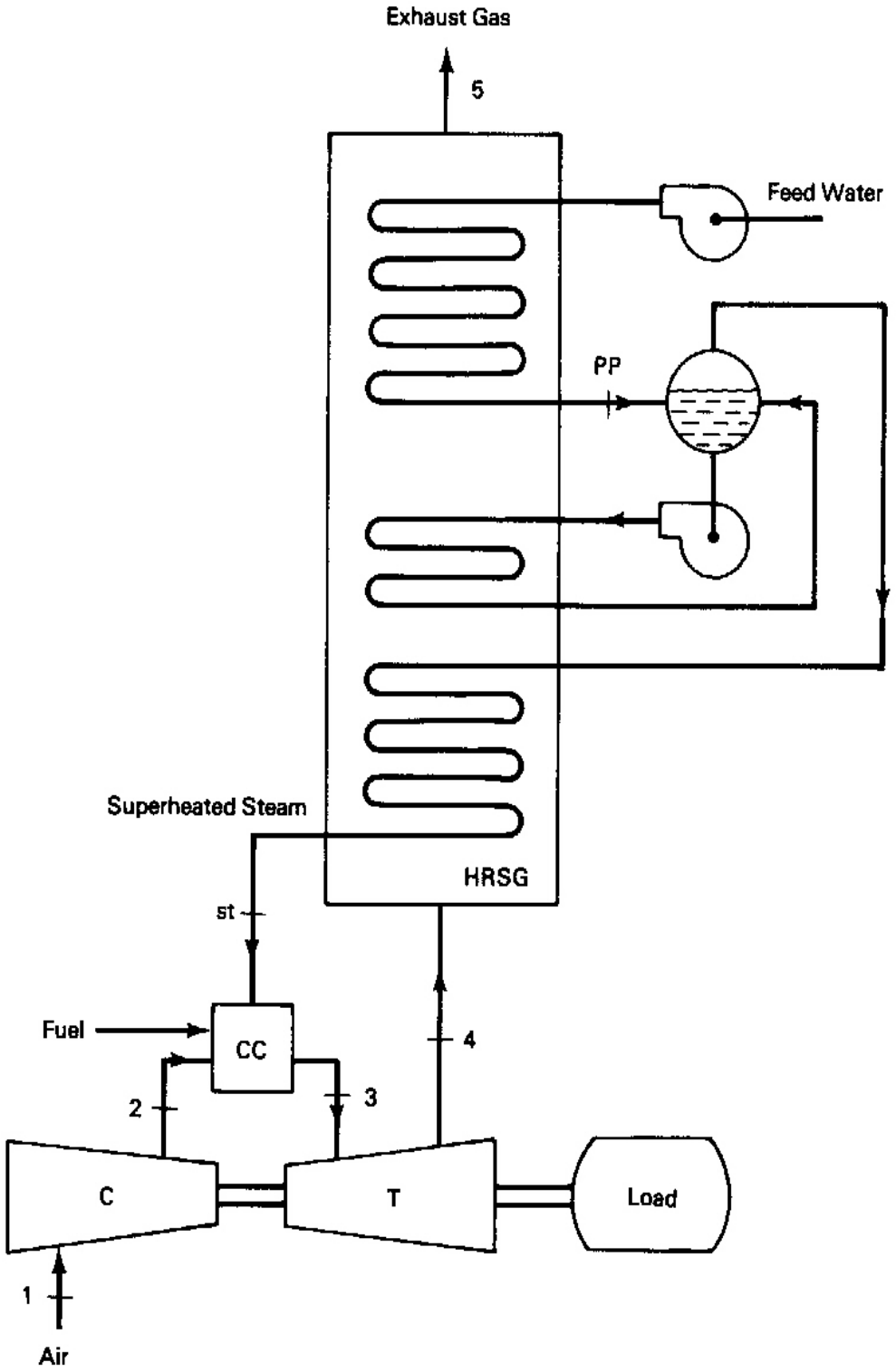


**FIGURE 9.22** Notation for steam-injected gas turbine analysis (Example 9.2).

heat capacity of steam in the turbine flow. The model assumes the following:

- Downstream steam injection has no effect on the compressor.

- The properties of steam may be represented by constant values of the heat capacity $C_{ps}$: 1.86 kJ/kg-K and 0.444 Btu / $lb_m$-R.

- The heat capacity of the mixture of combustion gas and steam may be represented by a temperature-independent mass-weighted heat capacity given by

$$C_{pm} = C_{pg} + (m_s/m_a)C_{ps} \qquad [\text{Btu/lb}_m\text{-R} \mid \text{kJ/kg-K}]$$

where $m_s/m_a$ is the steam-air mass ratio. Here, as before, the mass of fuel is neglected with respect to the mass of air.

- The isentropic exponent of the mixture, $k_m$, remains the isentropic exponent of combustion gas with no water injection, $k_m = k_g = 4/3$.

- The fuel control system maintains the turbine inlet temperature at a constant value, irrespective of steam injection rate.

## EXAMPLE 9.2

Consider the injection of steam in the combustion chamber of the single-shaft gas turbine studied in Example 5.1. Five pounds of steam are injected for every hundred pounds of compressor discharge air. The fuel flow rate is adjusted to maintain the turbine inlet temperature at a constant 1400°F. Compare the power output for a compressor flow rate of 100 $lb_m$/s, the thermal efficiency, the work ratio, and the fuel-air ratio with like parameters for the machine with no injection. Assume that the steam injected is saturated at the combustor pressure level and is heated by the turbine exhaust from pressurized feedwater at 70°F in a heat-recovery steam generator as shown in Figure 9.22.

### Solution

Table 9.5 presents the spreadsheet solution as well as the no-injection reference solution, which is repeated there for convenience.

The algorithm is based on the assumptions just enumerated and uses the HRSG analysis techniques discussed in section 9.2 in connection with the combined-cycle steam generator study. Steam conditions entering the combustor are obtained from the saturated-vapor tables, assuming constant pressure mixing at the known combustor pressure level; feed water conditions are for saturated liquid water at 70°F.

**TABLE 9.5** Spreadsheet Solution to Example 9.2

SIMPLE-CYCLE GAS TURBINE ANALYSIS
WITH STEAM-INJECTED GAS TURBINE MODIFICATION

| | | |
|---|---|---|
| REFERENCE CASE: | | |
| air isentropic exponent = k | 1.40 | given |
| (k-1)/k = e,a | 0.2857 | (k-1)/k |
| Heating value of fuel, Btu/lb | 20000 | |
| air mass flow rate, lb/sec | 100 | given |
| compressor inlet temperature = T1,R | 520.00 | given |
| compressor efficiency = etac | 0.86 | given |
| compressor pressure ratio = r | 6.00 | given |
| comp. isentropic exit temp. = T2s,R | 867.63 | T1r^e,a |
| compressor true exit temp. = T2,R | 924.22 | T1+(T2s-T1)/etac |
| compressor work = Wc,Btu/lb | -97.01 | 0.24(T1-T2) |
| comb. fractional pressure drop = fpl | 0.04 | given |
| turbine pressure ratio = rt | 5.76 | r(1-fpl) |
| turbine inlet temp = T3,R | 1860.00 | given |
| hot gas isentropic exponent = kg | 1.33 | given |
| (kg-1)/kg = e,g | 0.25 | (kg-1)/kg |
| gas heat capacity = cp,g, Btu/lb-R | 0.2744 | given |
| comb. heat addition = Qadded, Btu/lb | 256.78 | cp,g(T3-T2) |
| turb. isentropic exit temp. = T4s,R | 1200.63 | T3/(rt)^e,g |
| turb. isentropic efficiency = etat | 0.89 | given |
| turbine true exit temp. = T4,R | 1273.16 | T3-etat(T3-T4s) |
| turbine work = Wt,Btu/lb | 161.03 | cp,g(T3-T4) |
| net work = Wn,Btu/lb | 64.02 | Wt+Wc |
| thermal efficiency | 0.25 | Wn/Qa |
| work ratio | 1.66 | Wt/\|Wc\| |
| power output, KW | 6752.57 | 3600maWn/3413 |
| fuel-air ratio | 0.0128 | Qa/HV |
| | | |
| STIG MODIFICATION: | | |
| ms/ma | 0.05 | given |
| Cps, Btu/lb-R | 0.444 | given |
| Press. steam to combustor Pst, psia | 88.2 | 14.7(r) |
| Temp. of steam to combust. Tst, F | 319.5 | Lookup |
| Steam enthalpy. hst, Btu/lb | 1185.3 | Lookup |
| Feedwater temp. Tfw, F | 70 | given |
| hfw, sat liq. Btu/lb | 38.05 | Lookup |
| delta h for water in HRSG, Btu/lb | 1147.25 | hst - hfw |
| Ht trans in HRSG, Qhrsg, Btu/lb air | 57.36 | (ms/ma)delta h for water |
| hsat liq @ Pst, Btu/lb | 289 | Lookup |
| delta h liq. in econ. Dhl, Btu/lb | 250.95 | hsat liq. @ Ps - hfw |

*(continued on next page)*

**TABLE 9.5** (continued)

| | | |
|---|---|---|
| T3, R | 1860 | given |
| T3, F | 1400 | T3 (R) - 460 |
| hot gas isentropic exponent = kg | 1.33 | given |
| (kg-1)/kg = e,g | 0.25 | (kg-1)/kg |
| hot gas heat capacity cpg, Btu/lb-R | 0.2744 | given |
| Gas-steam ht cap. Cpm, Btu/lb air-R | 0.2966 | Cpg + (ms/ma)Cps |
| Qadded, Btu/lb-air | 280.77 | Cpg(T3-T2)+Cps(T3-Tst)ms/ma |
| turb. isentropic exit temp. = T4s,R | 1200.63 | T3/(rt)^e,g |
| turb. isentropic efficiency = etat | 0.89 | given |
| turbine true exit temp. = T4, R | 1273.16 | T3-etat(T3-T4s) |
| turbine work = Wt,Btu/lb air | 174.06 | Cpm(T3-T4) |
| net work = Wn,Btu/lb | 77.05 | Wt+Wc |
| thermal efficiency | 0.274 | Wn/Qadded |
| work ratio | 1.79 | Wt/;Wc! |
| power output, kW | 8126.74 | (3600/3413)maWn |
| fuel-air ratio | 0.0140 | Qadded/HV |
| HRSG exit temperature T5, R | 1079.76 | T4 - Qhrsg/Cpm |
| HRSG exit temperature T5, F | 619.76 | T4 (R) - 460 |
| Gas temp. at the pinchpoint, Tpp, F | 662.06 | T5 + (ms/ma)Dhl/Cpm |
| Pinchpoint temp. difference, F | 342.56 | Tpp - Tst |
| HRSG exit temp. difference, F | 549.76 | T5 - Tfw |
| HRSG inlet temp. difference, F | 493.66 | T4 - Tst |

A 3-point increase in thermal efficiency and a substantial increase in power output due to steam injection are evident.

The steam generator easily provides the required steam mass with a large pinchpoint temperature difference. This indicates that the turbine exhaust gas is capable of producing a still larger steam fraction with a smaller pinchpoint temperature difference while maintaining acceptable exhaust gas temperature with respect to the exhaust gas dew point.

---

By expanding the spreadsheet, with mass rate as a parameter, we present the influences of increased steam mass rate on performance and on steam generator steam-air temperature differences in Figures 9.23 and 9.24, respectively. The figures indicate that steam-air mass ratios up to about 0.18 are possible with this configuration and that substantial performance benefits are the result.

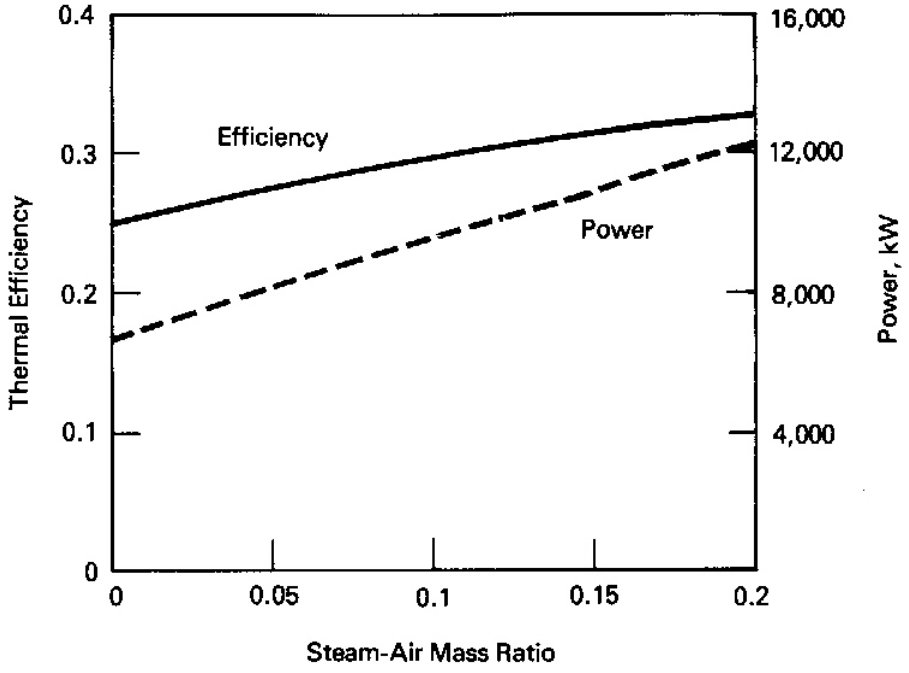


**FIGURE 9.23** Steam-injected gas turbine performance.

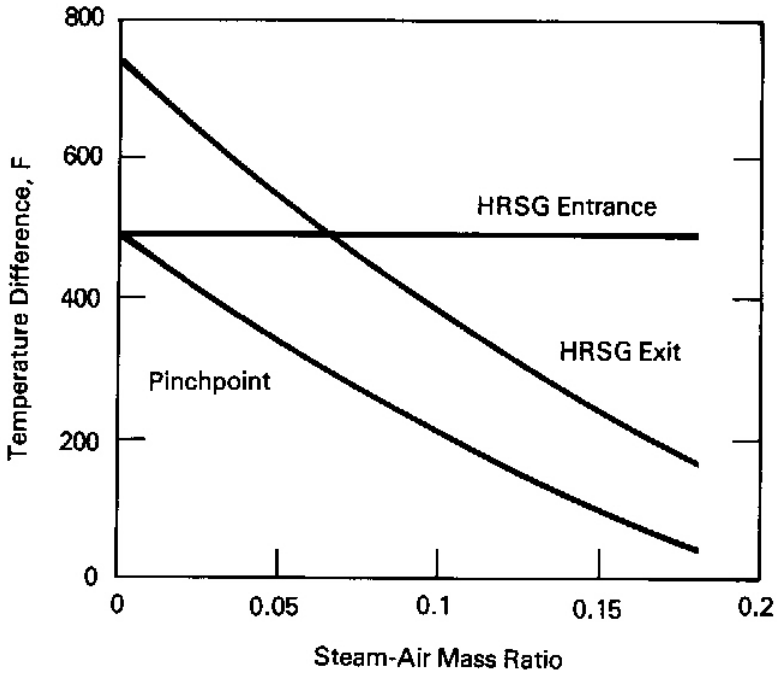


**FIGURE 9.24** Gas–steam temperature differences.

FIGURE 9.25 Modern resource recovery facility. (Courtesy of Ogden Martin Systems, Inc.)

## 9.9 Resource Recovery

The disposal of municipal and industrial solid waste has become a national concern with significant energy conversion aspects. It has been estimated that 50% of sanitary landfills that are convenient or accessible to urban areas would be fully utilized in the 1990s and that satisfactory new sites will be progressively more difficult to find. This has led to the rapid growth of the resource recovery industry.

*Resource recovery* deals with the environmentally sound disposal of municipal and industrial waste. It starts, at one extreme, with garbage landfills and incineration and extends to the ultimate conversion of components of waste to their useful constituent elements, with recovery of available energy in the process. Vigorous activity in this area is producing a variety of approaches to the problem. Many of the solutions focus on the development of a central waste disposal facility that receives and prepares waste for efficient landfill disposal. This section considers a modern facility that reduces the volume of about 1125 tons per day of solid waste by over 90% by burning, to produce steam for industrial use and to generate electricity when steam is not needed.

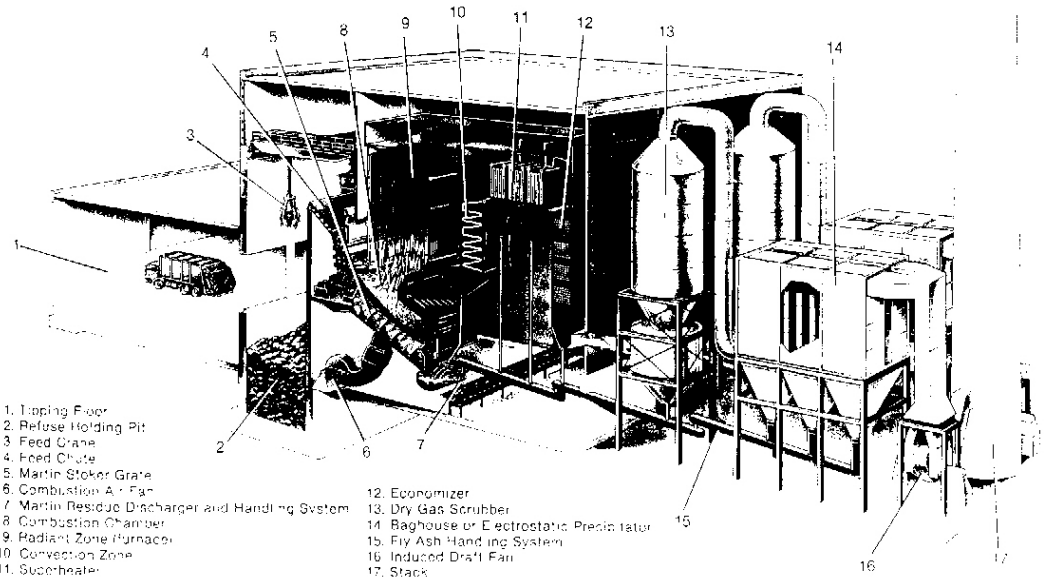


**FIGURE 9.26** Schematic of a steam generating waste disposal facility. (Courtesy of Ogden Martin Systems, Inc.)

Figure 9.25 shows a modern facility designed to serve the waste disposal needs of almost 500,000 Tulsa-area residents. The plant is similar in many respects to the power plant steam generators discussed earlier. Major exceptions are the modifications required to deal with the unique problems of handling municipal solid waste (MSW). The right foreground of Figure 9.25 shows where waste haulers' trucks are weighed on outside scales and enter the facility's tipping floor. Large noncombustible materials and other refuse that cannot be burned in the facility, such as steel bars and tires, are left outside the plant by the hauler for separate disposal. The trucks dump the MSW in or near a large refuge storage pit adjacent to the tipping floor and leave from the opposite side of the tipping floor from which they entered.

Haulers are held responsible for the waste that they deliver, although overhead crane operators who feed refuse to the three boilers also attempt to sort the refuse, to help achieve uniform heat release in the furnace and to keep large, noncombustible, hazardous, and otherwise inappropriate materials from entering the furnaces.

Figure 9.26 shows how refuse handled by cranes is hoisted from the holding pit and lowered through near-vertical feed chutes (4) to inclined reciprocating-grate furnaces (5). There, rugged hydraulically operated rams meter the flow of refuse as they push it onto the grates. The combination of underfire air from a forced-draft fan (6) and vertically reciprocating grates keeps the refuse in continuous motion. Overfire air assures 98% burnup of combustible materials. Supply air for the forced-draft fans is drawn from the tipping-floor enclosure (1), to retain odors within the plant.

At the end of the grate, a variable-speed ash discharge roller controls the rate of discharge and hence the depth of the ash bed at the end the grate. The ash falls

from the roller into a water-bath ash discharger that cools the residue. The water also seals the bottom of the furnace, which is slightly below atmospheric pressure. The cooling ash residue is pushed by a ram out of the water bath, up an inclined surface, and into a compartment where water is allowed to drain off and evaporate from the residue for fifteen minutes. The ash residue then falls to a conveyor, where it is transported to the ash house. There, salvageable metals are separated and recycled. The remaining ash is then trucked to a sanitary landfill. The plant achieves about a 90% reduction in refuse volume delivered to the landfill.

In the furnaces, the combustion gas from the burning MSW on the grates heats the water in the welded-membrane water walls of the furnaces and the various steam generator tube banks (8-12). Each of the steam generators produces 88,500 $lb_m$/hr of steam at 680 psia and 700°F. The entire steam production passes in a 12-inch underground steam line to a refinery about a mile away, for process use. In figure 9.25, the refinery process plant utilizing the steam is located just beyond the tank farm in the upper left. A steam turbine and generator set rated at 16 MW is available for electrical generation as an alternative to refinery use of steam production. The electricity may be used on site or sold to the local electric utility.

After leaving the economizer (12), combustion gas passes into an electrostatic precipitator (14), where most of the fly ash remaining from the numerous passes through the boiler is collected. The precipitators have automatic rapping systems that free the collected particles, allowing them to drop into flyash hoppers to be transported to the residue conveyor. Induced-draft fans (16) transport the cleaned combustion gas from the precipitators to the stacks.

Tulsa's Walter B. Hall Resource Recovery Facility, described here, is an environmentally sound example of an increasing number of facilities operating or under construction. These facilities typically are externally neat and are suited for operation in industrial and some commercial locations. Massive reductions in waste volumes are achieved in these facilities, with the possibility of generating steam for process use, district heating, and steam turbine generation of electricity. In resource recovery facilities of differing design, fluidized bed combustors might be employed, and the released refuse heat might instead be used in connection with closed-cycle gas turbines or other heat-driven devices.

## 9.10 Polytropic Efficiency

To this point the performance of turbomachinery has been represented by isentropic efficiencies. In comparisons of turbomachines with differing pressure ratios, the use of the isentropic efficiency gives an undeserved advantage to some machines over others with different pressure ratios. Another approach to efficiency, called the *small-stage efficiency* or *polytropic efficiency*, is considered here as an alternative and, under certain circumstances, a more consistent way of representing the quality of turbine and compressor performance.

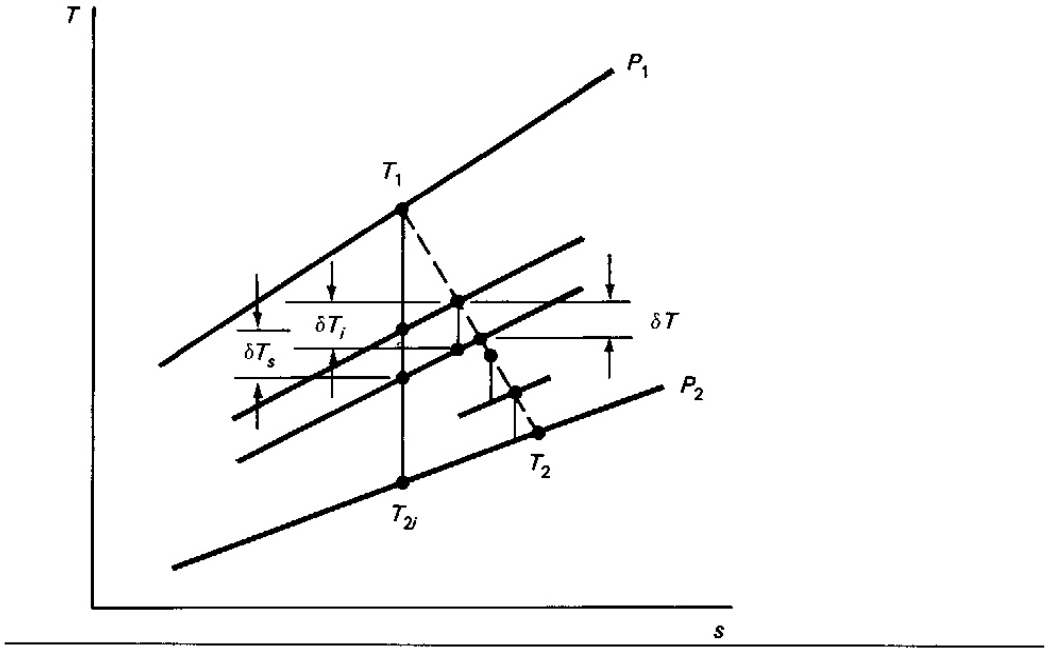


**FIGURE 9.27** Temperature–entropy diagram for a small turbine stage.

Axial compressors and turbines consist of alternating rows of stationary, or *stator,* blades and rotating, or *rotor*, blades, with the rotor rows firmly attached to a rotating shaft. In a turbine, the stationary blades act as nozzles to increase flow velocity, and the rotor blades downstream turn and decelerate (change the momentum of) the flow. The reaction to the momentum change is a force with a large component in the direction of blade rotation. This blade force delivers torque and power about the rotor axis. The combination of the stator row and a rotor row is called a *stage*.

Instead of thinking in terms of efficiency for the entire machine, we focus our attention on the efficiency of a single turbine stage. The efficiency of a stage may be defined in terms analogous to the definition of the isentropic efficiency. Consider the T-s diagram of Figure 9.27, which shows the temperature drop of a calorically perfect gas in a stage of a multistage turbine. We assume here that all stages have identical pressure ratios. In the notation of the figure, the turbine isentropic efficiency is given by $(T_1 - T_2)/(T_1 - T_{2i})$, and by analogy the *stage isentropic efficiency* is $\delta T/\delta T_i$.

The expansion process in the turbine may be thought of as a stairstep sequence of expansions through individual small stages, each having its own efficiency. A few such steps are indicated in the figure. It should be observed that, in each successive stage, the isentropic temperature drop $\delta T_i$ moves to the right on the diagram and therefore is larger than the corresponding drop between the same pressure levels on the expansion line from 1 to 2i; i.e., $\delta T_i > \delta T_s$. Thus the irreversibility of the expansions through earlier stages results in a sum of stage isentropic temperature drops greater than the overall isentropic temperature drop and hence greater work-producing capability for successive stages.

Let us now imagine the turbine as comprised of an infinite number of stages with infinitesimal pressure drops of equal efficiency. Thus the $\delta T$s become d$T$s and the *small-stage efficiency* becomes

$$\eta_s = dT/dT_i \qquad \text{[dl]} \qquad (9.7)$$

The isentropic relation for a calorically perfect gas, Equation (1.19), may be written in the form $T/p^{(k-1)/k}$ = a constant. Using differentiation by parts yields

$$dT_i - [(k-1)/k]Tp^{-1}dp = 0$$

which combined with Equation (9.7), gives

$$dT/T = [\eta_s (k-1)/k]\, p^{-1}dp \qquad \text{[dl]} \qquad (9.8a)$$

If it is assumed that the stage efficiency is constant, integration of Equation (9.8a) between the turbine inlet and exit states gives

$$T_1/T_2 = (p_1/p_2)^{\eta_s (k-1)/k} \qquad \text{[dl]} \qquad (9.8b)$$

Thus the requirement that all stages have equal efficiency yields a temperature pressure relationship of the same form as Equation (1.19), except for the exponent. Such relationships, of the form $T_1/T_2 = (p_1/p_2)^{(n-1)/n}$ are called polytropic. For example, the isentropic Equation (1.19) is polytropic with $n = k$. Because the use of constant small-stage efficiency yields a pressure-temperature relation of polytropic form, $\eta_s$ is often called the *polytropic efficiency*. The exponent for the turbine expansion with constant stage efficiency is then given by

$$(n-1)/n = \eta_s(k-1)/k \qquad \text{[dl]} \qquad (9.9)$$

If the polytropic efficiency is unity, $n$ becomes $k$, and Equations (9.8) become the usual isentropic relation. Values of $\eta_s$ less than 1 reduce the turbine temperature ratio, $T_1/T_2$, for a given turbine pressure ratio, $p_1/p_2$, below the isentropic value in qualitatively the same way that decreasing turbine isentropic efficiency does. A similar statement applies to turbine work.

The turbine isentropic efficiency, $\eta_t$, can be expressed in terms of the polytropic efficiency by substitution in the isentropic efficiency definition:

$$\eta_t = (T_2/T_1 - 1)/(T_{2i}/T_1 - 1)$$

$$= (1/r^{\eta_s(k-1)/k} - 1)/\,(1/r^{(k-1)/k} - 1) \qquad \text{[dl]} \qquad (9.10)$$

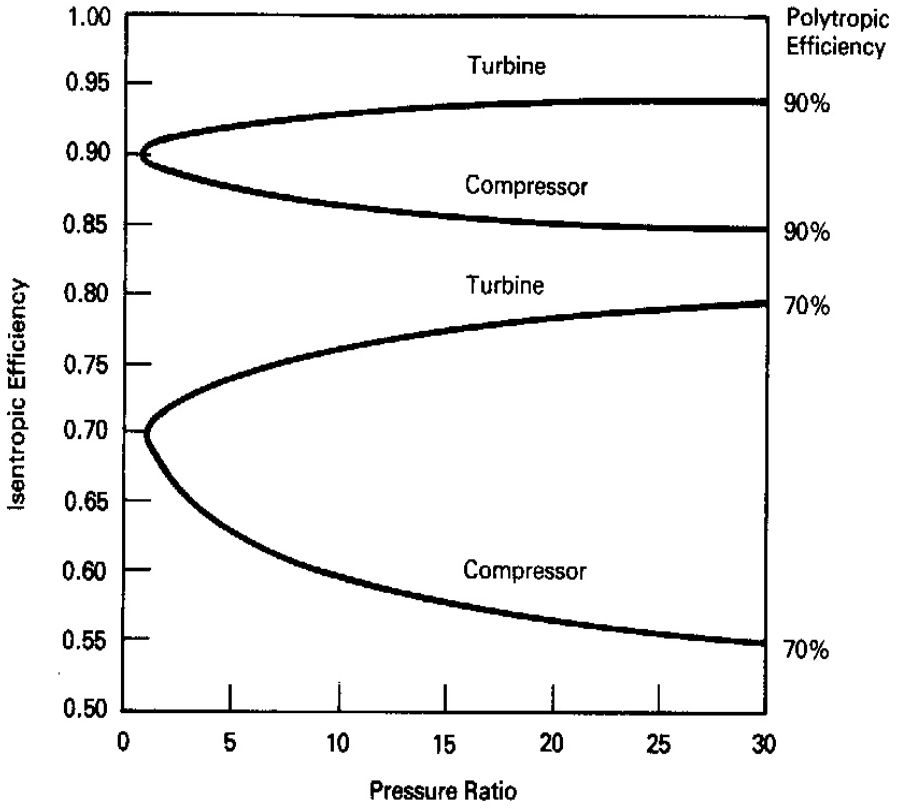


**FIGURE 9.28** Relationship between isentropic and polytropic efficiencies.

where $r$ is the turbine pressure ratio, $p_1/p_2$.

If we define a compressor polytropic efficiency as a small-stage isentropic efficiency, a similar analysis yields relations analogous to Equations (9.8) – (9.10):

$$T_2/T_1 = (p_2/p_1)^{(k-1)/(k\eta_s)} \quad [dl] \tag{9.11}$$

$$(n-1)/n = (k-1)/(k\eta_s) \quad [dl] \tag{9.12}$$

$$\eta_c = (r^{(k-1)/k} - 1)/(r^{(k-1)/(k\eta_s)} - 1) \quad [dl] \tag{9.13}$$

where $\eta_c$ and $r$ are the compressor isentropic efficiency and pressure ratio, respectively. Figure 9.28 shows isentropic efficiencies for both compressors and turbines as functions of pressure ratio for two values of polytropic efficiencies. Applying L'Hospital's rule to Equations (9.10) and (9.13), we can show that the isentropic efficiency of both turbines and compressors approaches the polytropic efficiency in the limit as the pressure ratio approaches 1. This fact is evident in the figure, and it is apparent that as pressure ratio increases, isentropic efficiencies increase for turbines and decrease for compressors for fixed values of the polytropic efficiencies.

The polytropic efficiencies may be regarded as measures of the internal quality of turbomachines, that is, superior internal blade passage design. For example, for two turbines having the same internal aerothermodynamic quality, Figure 9.28 indicates that a machine with a high pressure ratio will have a higher overall isentropic efficiency than one with a low pressure ratio.

As another example, the compressor curves imply that, in a comparison of two compressors having the same isentropic efficiency, the one with the higher pressure ratio has a superior aerothermodynamic quality. This suggests that parametric studies involving varying compressor pressure ratio should use a constant value of polytropic efficiency rather than constant isentropic efficiency to represent comparable compressor quality.

## 9.11 Turbofan Engines

The turbofan engine, ducted fan, or fanjet, discussed briefly in Chapter 5, is the dominant gas turbine engine in commercial aircraft and is extensively employed in military aircraft is well. Its primary feature is a large fan that accelerates a large mass of unheated air in an annular duct surrounding the central core engine, as in Figures 9.29 and 9.30, which show, respectively, a cutaway diagram and a photograph of the General Electric CF6-80C2 high-bypass-ratio engine. The large fan diameter produces a large jet exhaust consisting of a cylindrical wake of hot combustion gas surrounded by an annular flow of slower-moving warm air.

The *bypass ratio*, $B$, is the ratio of the mass flow rate through the outer cooler duct, $m_c$, to the flow rate of the hot core engine, $m_h$:

$$B = m_c/m_h \qquad [\text{dl}] \qquad (9.14)$$

Bypass ratios range from 0 for the pure turbojet engine studied in Chapter 5 to values in the neighborhood of 10. The bypass ratio is a design parameter that is primarily determined by the mission of the aircraft. High-bypass-ratio engines are desirable for long-range commercial aircraft because of their excellent fuel economy. The CF6-80C2 engine has a bypass ratio of 5.05 and a total airflow of 1769 $lb_m/s$ (802 kg/s).

The bypass air may have its own nozzle, separate from the core engine as in the CF6 engine, or the core and bypass flows may be mixed in a specially designed nozzle. The mixing nozzle helps to reduce jet noise by transferring momentum from the fast-moving core gas to the slower-moving bypass air, thereby reducing the wake shear noise source. The mixing process, however, involves a thrust-loss penalty.

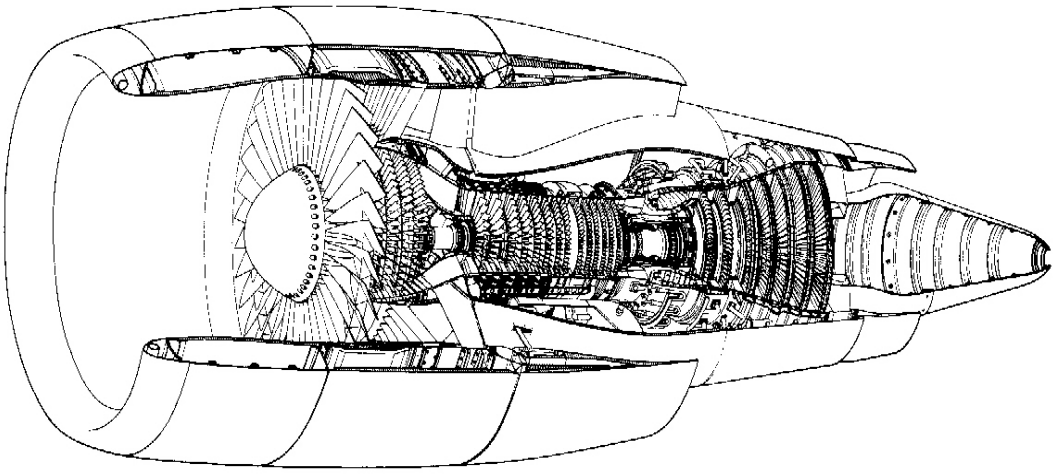

**FIGURE 9.29** Cutaway of the CF6-80C2 turbofan engine in a Nacelle installation. The entire air flow passes through the fan at the left. About one-fifth of the flow passes through the compressor, the combustor, and the turbines and the balance through the bypass duct. (Courtesy of GE Aircraft Engines.)

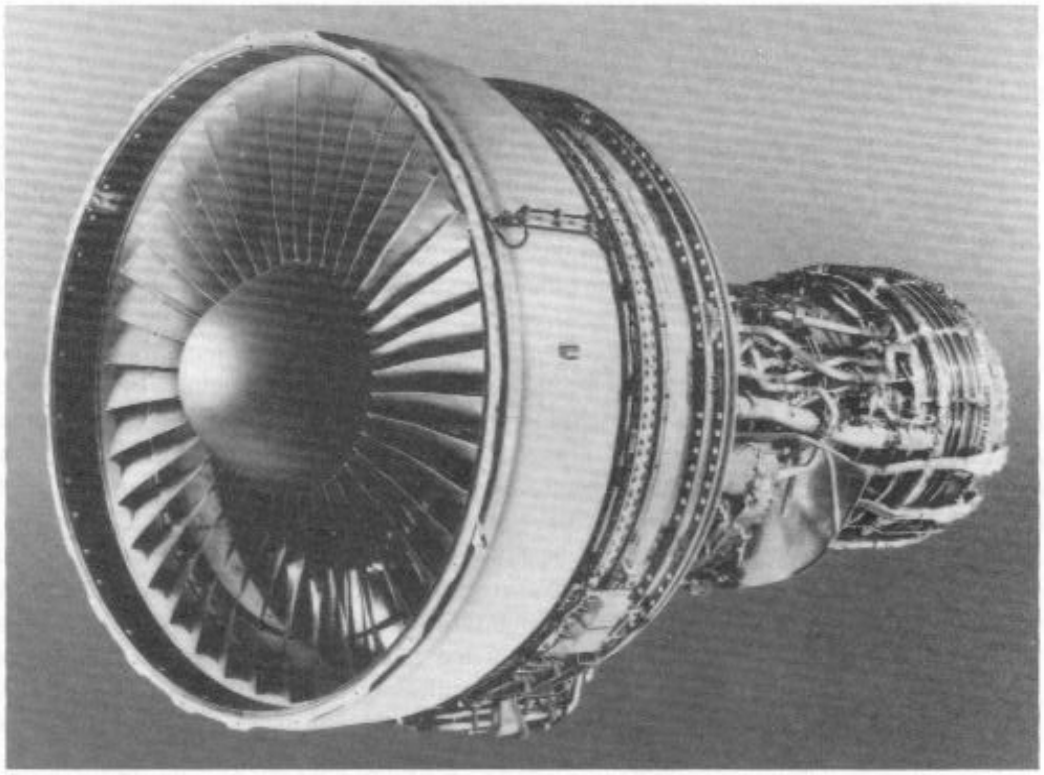

**FIGURE 9.30** CF6-80C2 high-bypass-ratio turbofan engine used in Boeing 747 and 767, McDonnell-Douglas MD-11, and other aircraft. (Courtesy of GE Aircraft Engines.)

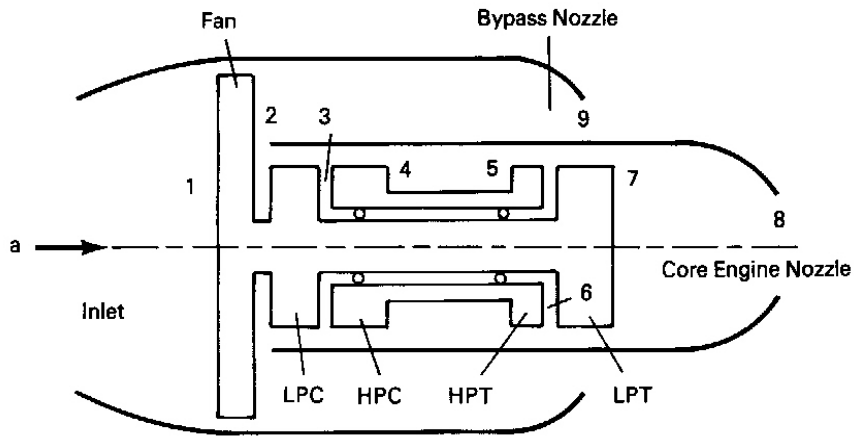


**FIGURE 9.31** Thermodynamic stations and nomenclature for turbofan analysis: F = fan, LPC = low-pressure compressor, HPC = high-pressure compressor, HPT = high-pressure turbine, LPT = low-pressure turbine.

Figure 9.31 presents some of the nomenclature and notation that will be used in discussing the turbofan engine. For the configuration shown in the figure, the fan pressurizes the compressor inlet air as well as delivering the power needed to accelerate the bypass air through its nozzle downstream. While other fan configurations are possible, this frequently used arrangement is the only one analyzed here.

In addition to the bypass ratio, a second important design parameter is the *fan pressure ratio*, the ratio of the stagnation pressure downstream to that upstream of the fan:

$$\text{FPR} = p_{o2}/p_{o1} \qquad [\text{dl}] \qquad (9.15)$$

The fan pressure ratio, together with the bypass ratio, determines the power transferred between the hot core engine and the bypass flow. For a given core engine configuration, higher bypass ratios and fan pressure ratios cause more power to be extracted from the turbine and passed to the bypass air by the fan. This produces higher bypass duct thrust. However, as more power is extracted from the core flow, the core nozzle velocity and core engine thrust are reduced. The determination of the design values of these parameters therefore involves a complex tradeoff with numerous other design factors.

The combination of a compressor and a turbine joined by a shaft is sometimes referred to as a spool. High-pressure-ratio engines are frequently arranged in a twin-spool or even a three-spool configuration. In a twin-spool engine, a high-pressure turbine drives a high-pressure compressor with a hollow shaft, and a low-pressure turbine delivers power to a low-pressure compressor and/or a fan by means of a shaft that turns inside of the high-pressure-spool shaft. The turbofan configuration in Figure 9.31 has the low-pressure turbine driving both the fan and

the low-pressure compressor, as does the PW 4000 fanjet shown in Figure 5.24. In another arrangement, the low pressure turbine powers the fan only, and the entire compressor is driven by the high-pressure turbine. Regardless of engine layout, the objective of the fanjet is to accelerate a large mass of air and thereby increase the propulsive efficiency of the engine.

Let us now consider the analysis of the turbofan configuration shown in Figure 9.31. The following parameters are assumed to be specified:

- Ambient conditions at a specified altitude and flight speed or Mach number, $p_a$, $t_a$, $c_a$, or $M_a$
- Inlet stagnation-pressure recovery, IPR
- High-pressure-turbine inlet stagnation temperature, $T_{o5}$
- Fan pressure ratio, FPR = $p_{o2}/p_{o1}$
- Bypass ratio, $B$
- Low-pressure-compressor pressure ratio, LPCPR = $p_{o3}/p_{o2}$
- High-pressure-compressor pressure ratio, HPCPR = $p_{o4}/p_{o3}$
- Low- and high-pressure compressor efficiencies, $\eta_{LPC}$, $\eta_{HPC}$
- Low- and high-pressure turbine efficiencies, $\eta_{LPT}$, $\eta_{HPT}$
- Fan efficiency, $\eta_F$ (defined analogous to compressor efficiency)

The inlet is assumed adiabatic, the nozzles are assumed to be isentropic, and all mechanical efficencies are taken to be unity.

The calculation procedure parallels that of the turbojet analysis of Chapter 5. Free-stream stagnation conditions are determined from the ambient conditions and flight speed or Mach number. For an adiabatic inlet, the stagnation temperature at the fan face, $T_{o1}$, is the same as the free-stream value, $T_{oa}$, and the fan face stagnation pressure, $p_{o1}$, is given by the product of the inlet stagnation-pressure recovery and the free-stream stagnation pressure: $p_{o1} = \text{IPR} \cdot p_{oa}$.

The conditions immediately downstream of the fan, assumed to be the same for both hot and cold paths, are given by

$$p_{o2} = p_{o1} \cdot \text{FPR} \qquad [\text{lb}_f/\text{in}^2 \mid \text{kPa}] \qquad (9.16)$$

and

$$T_{o2} = T_{o1} + T_{o1}[\text{FPR}^{(k-1)/k} - 1]/\eta_F \qquad [\text{R} \mid \text{K}] \qquad (9.17)$$

The pressurized flow in the bypass duct then accelerates from $p_{o2}$ and $T_{o2}$ through the convergent nozzle to a high velocity $c_9$ with static pressure $p_9$, contributing $m_9(c_9 - c_a) + A_9(p_9 - p_a)$ to the engine thrust. Here, $p_9 = p_a$ if the nozzle pressure ratio, $p_{o2}/p_9$, is less than or equal to the critical pressure ratio; otherwise it is equal to the critical pressure ratio.

The stagnation conditions downstream of both low- and high-pressure compressors are determined in the same way as for the fan. For instance, for the low-pressure compressor,

$$p_{o3} = p_{o2} \cdot \text{LPCPR} \qquad [\text{lb}_f/\text{in}^2 \mid \text{kPa}] \qquad (9.18)$$

and

$$T_{o3} = T_{o2} + T_{o2}[\text{LPCPR}^{(k-1)/k} - 1]/\eta_{\text{LPC}} \qquad [\text{R} \mid \text{K}] \qquad (9.19)$$

Similarly, for the high-pressure compressor,

$$p_{o4} = p_{o3} \cdot \text{HPCPR} \qquad [\text{lb}_f/\text{in}^2 \mid \text{kPa}] \qquad (9.20)$$

and

$$T_{o4} = T_{o3} + T_{o3}[\text{HPCPR}^{(k-1)/k} - 1]/\eta_{\text{HPC}} \qquad [\text{R} \mid \text{K}] \qquad (9.21)$$

Neglecting combustor pressure losses, the high-pressure-turbine inlet pressure is $p_{o5} = p_{o4}$ and the known turbine inlet temperature is $T_{o5}$. Recognizing that, apart from assumed-small frictional losses, the power delivered by the high-pressure turbine is delivered to the high-pressure compressor; the steady-flow form of the First Law of Thermodynamics applied to the high-pressure spool yields the stagnation temperature upstream of the low-pressure turbine:

$$m_8 C_{pa}(T_{o4} - T_{o3}) = m_8 C_{pg}(T_{o5} - T_{o6})$$

$$T_{o6} = T_{o5} - (C_{pa}/C_{pg})(T_{o4} - T_{o3}) \qquad [\text{R} \mid \text{K}] \qquad (9.22)$$

The turbine isentropic efficiency definition then gives the isentropic discharge temperature, $T_{o6s}$, which in turn yields the high-pressure-turbine pressure ratio.

A similar procedure for the low-pressure turbine spool results in the energy rate balance:

$$(m_9 + m_8)C_{pa}(T_{o2} - T_{o1}) + m_8 C_{pa}(T_{o3} - T_{o2}) = m_8 C_{pg}(T_{o6} - T_{o7}) \qquad [\text{Btu/hr} \mid \text{kW}]$$

which, after dividing by $m_8 C_{pa}$ and using the bypass ratio equation, yields

$$(\text{B} + 1)(T_{o2} - T_{o1}) + (T_{o3} - T_{o2}) = (C_{pg}/C_{pa})(T_{o6} - T_{o7}) \qquad [\text{R} \mid \text{K}]$$

This equation may be solved for the nozzle entrance stagnation temperature:

$$T_{o7} = T_{o6} - (C_{pa}/C_{pg})[(B + 1)(T_{o2} - T_{o1}) + (T_{o3} - T_{o2})] \quad [R \mid K] \tag{9.23}$$

The turbine pressure ratio follows from the application of the isentropic turbine efficiency definition and the isentropic temperature-pressure relation, as in the earlier high-pressure-turbine analysis.

Alternatively, *polytropic efficiencies* may be used in the solutions. This is done for the fan and compressors by replacing Equations (9.16) to (9.21) by their polytropic equivalents:

$$p_{o2} = p_{o1} \cdot FPR \quad [lb_f/in^2 \mid kPa] \tag{9.24}$$

$$T_{o2} = T_{o1} + T_{o1}[FPR^{(n-1)/n} - 1] \quad [R \mid K] \tag{9.25}$$

$$p_{o3} = p_{o2} \cdot LPCPR \quad [lb_f/in^2 \mid kPa] \tag{9.26}$$

$$T_{o3} = T_{o2} + T_{o2}[LPCPR^{(n-1)/n} - 1] \quad [R \mid K] \tag{9.27}$$

$$p_{o4} = p_{o3} \cdot HPCPR \quad [lb_f/in^2 \mid kPa] \tag{9.28}$$

$$T_{o4} = T_{o3} + T_{o3}[HPCPR^{(n-1)/n} - 1] \quad [R \mid K] \tag{9.29}$$

where $(n - 1)/n$ is given by Equation (9.12) for the appropriate compressor poltytropic efficiency.

Equations (9.22) and (9.23) are still applicable for the analysis of the turbines. However, polytropic equations, using exponents given by Equation (9.9):

$$n/(n - 1) = k/(k - 1)\eta_s$$

where $\eta_s$ is the appropriate turbine polytropic efficiency, are required to determine the turbine pressure ratios, namely

$$p_{o6}/p_{o5} = (T_{o6}/T_{o5})^{n/(n-1)} \quad [dl] \tag{9.30}$$

and

$$p_{o7}/p_{o6} = (T_{o7}/T_{o6})^{n/(n-1)} \quad [dl] \tag{9.31}$$

Once $p_{o7}$ and $T_{o7}$ are known, the core nozzle may be treated in the same way as the turbojet nozzle in Chapter 5. The engine thrust is then the sum of the thrusts produced by the core and bypass flows.

**EXAMPLE 9.3**

A turbofan engine has a fan and a low-pressure compressor driven by the low-pressure turbine, as shown in Figure 9.31. It operates at a flight velocity of 200 m/s at 12,000 meters altitude, where the ambient temperature and pressure are 216.65K and 0.1933 bar, respectively. The overall pressure ratio the engine is 19, and the fan and low-pressure-compressor pressure ratios are 1.65 in 2.5, respectively. The fan, compressors, and turbines have 90% polytropic efficiencies. Assume an isentropic inlet and separate isentropic convergent nozzles, a fuel heating value of 43,000 kJ/kg, and a combustor total pressure loss of 6.5%.

Determine the core engine and bypass duct exit velocities, the engine thrust specific fuel consumption, thrust, and specific thrust for an engine with an inlet air flow of 100 kg/s and a bypass ratio of 3.0. Determine whether the nozzles are choked.

Solution

Table 9.6 tabulates, in spreadsheet format, the design data for the example and systematically calculates the engine parameters. After computing the fan and LP-turbine exit total pressures, the nozzles may be checked for choking at the throats. The applied pressure ratios are compared with the critical pressure ratios for cold bypass air ($k = 1.4$) and for hot gas ($k = 4/3$), respectively. Branching in the computation required by the presence or absence of choking is easily handled by the @IF function of popular spreadsheets, which allows a conditional selection between specified alternatives, as discussed previously in connection with Example 5.6.

TABLE 9.6 Spreadsheet Solution to Example 9.3

AEROTHERMODYNAMIC ANALYSIS OF A FANJET

| | | |
|---|---|---|
| Ca | 200 m/s | Flight velocity |
| Ta | 216.65 K | Ambient temperature |
| Pa | 0.1933 Bar | Ambient pressure |
| Fuel HV | 43000 kJ/kg | Heating value |
| Cpa | 1.005 kJ/kg | Air heat capacity |
| Cpa/Cpg | 0.8754 | Air/gas heat capacity ratio |
| OPR | 19.0000 | Overall pressure ratio |
| FPR | 1.6500 | Fan pressure ratio |
| LPCPR | 2.5000 | Low pressure compressor pressure ratio |
| HPCPR | 4.6100 | HPCPR = OPR/[(FPR)(LPCPR)] |
| B | 3.0000 | Bypass Ratio |
| mair | 100 kg/s | Inlet total mass flow rate |
| cpeta | 0.9 | Compressor and fan polytropic efficiencies |
| (n-1)/n l comp | 0.3175 | (n-1)/n = (k-1)/[k•cpeta] (for fan & comp.) |

| | | |
|---|---|---|
| tpeta | 0.9 | Turbine polytropic efficiency |
| n/(n-1) l turbine | 4.4400 | Turbine polytropic factor, k/[(k-1)•tpeta] |
| (dp/p) l combust | 0.065 | Combustor fractional pressure drop |
| To5 | 1027 C | High pressure turbine inlet temperature |
| To5 | 1300 K | To5 (K) = To5 (C) + 273 |
| To1=Toa | 236.550 K | Toa=Ta+Ca^2/(2•Cpa*1000) |
| Poa = Po1 | 0.263 Bar | Po1 = Poa = Pa•(Toa/Ta)^3.5 |
| Po2 | 0.434 Bar | Po2=FPR•Po1 |
| Po3 | 1.085 Bar | Po3=(LPCPR)Po2 |
| Po4 | 4.995 Bar | Po4=Po3(HPCPR) |
| Po5 | 4.671 Bar | Po5=Po4•[1 - (dp/p)] \| combust |
| To2 | 277.31 K | To2=To1•FPR^[(n-1)/n] l comp |
| To3 | 370.93 K | To3=To2•(LPCPR)^[(n-1)/n] \| comp |
| To4 | 602.39 K | To4=To3•HPCPR^[(n-1)/n] \| comp |
| To6 | 1097.38 K | To6=To5-(Cpa/Cpg)•(To4-To3) |
| To7 | 872.68 K | To7=To6-(Cpa/Cpg)[(B+1)(To2-To1)+(To3-To2)] |
| Po6 | 2.199 Bar | Po6=Po5•(To6/To5)^[n/(n-1)] \| turbine |
| Po7 | 0.795 Bar | Po7=Po6•(To7/To6)^[n/{n-1)] \| turbine |
| Po7/Pc8 | 1.8530 | Crit. press. ratio: Po7/Pc8=[(4/3+1)/2]^4 |
| Po7/Pa | 4.1100 | Core flow is choked |
| Po2/Pc9 | 1.8930 | Crit. Press. ratio: Po2/Pc9=[(7/5+1)/2]^3.5 |
| Po2/Pa | 2.2440 | Bypass flow is choked |
| T8 | 748.02 K | IF (Po7/Pc8) < (Po7/Pa) THEN T8=2•To7/(4/3+1) ELSE T8=To7/(Po7/Pa)^0.25 |
| C8 | 535.02 m/s | IF (Po7/Pc8)<(Po7/Pa) THEN C8=(287•T8•4/3)^0.5 ELSE C8 = [(To7-T8)•2000•Cpg)]^0.5 |
| P8 | 0.429 Bar | IF Pc8>Pa THEN P8=Po7/(Po7/Pc8) ELSE P8=Pa |
| Rho8 | 0.200 kg/m^3 | Rho8=100•P8/(0.287*T8) |
| A8/m8 | 0.0094 m^2-s/kg | A8/m8 = 1 / (C8•Rho8) |
| T9 | 231.09 K | IF Pc9>Pa THEN T9=2To2/(7/5+1) ELSE T9=To2/(Po2/Pa)^(1/3.5) |
| C9 | 304.72 m/s | IF Pc9>Pa THEN C9=(287•T8•7/5)^0.5 ELSE C=[(To2-T9)•2000•Cpa]^0.5 |
| P9 | 0.229 Bar | IF Pc9>Pa THEN P9=Po2/(Po2/Pc9) ELSE P9=Pa |
| rho9 | 0.346 kg/m^3 | Rho9=100•P9/(0.287•T9) |
| A9/m9 | 0.009 m^2-s/kg | A9/m9=1 / (C9•Rho9) |
| Specific Thrust, ST | 242.9 N-s/kg | ST = C8+C9•B-Ca•(B+1)+[(P8-Pa)•(A8/m8) +(P9-Pa)•(A9/m9)•B]•10^5/(B+1) |
| Thrust | 24294.4 N | Total engine thrust= mair(specific thrust) |
| f/a | 0.0186 | f/a=Cpg(To5-To4)/HV |
| mfuel | 0.466 kg/s | Fuel flow rate=mair•(f/a)/(B+1) |
| TSFC | 0.000019 kg/N-s | TSFC=(f/a)/[spec. thrust)(B+1)] |
| TSFC' | 0.069 kg/N-hr | TSFC'=3600•TSFC |
| ST \| core m | 971.8 N-s/kg | ST based on m8 = (B+1)•ST |

The specific thrust is presented in two forms, one based on the total mass flow rate to the engine and the other based on the mass flow rate to the core engine. The former, ST, allows easy comparison with engines of comparable frontal area, while the latter, ST | core m, is useful in showing the thrust increase due to adding

a fan to a given core engine. Both definitions reduce to the common turbojet definition for $B = 0$, but deviate progressively with increasing bypass ratio.

---

It is of interest to compare the performance of a turbofan and twin-spool turbojet in flight at the same altitude and velocity based on our computations. This is easily accomplished with the spreadsheet of Table 9.6 by setting FPR = 1.0 and $B = 0$ for the turbojet engine. Table 9.7 shows some of the parameters resulting from this comparison.

Table 9.7 Turbofan–Turbojet Comparison

| | **Turbofan** | **Turbojet** |
|---|---|---|
| Core jet velocity, m/s | 535.02 | 566.88 |
| Bypass jet velocity, m/s | 304.72 | --------- |
| Thrust, N | 24,294.4 | 67,745 |
| Specific thrust based on total mass, N-s/kg | 242.9 | 677.5 |
| Specific thrust based on core mass, N-s/kg | 971.8 | 677.5 |
| Fuel mass flow rate, kg/s | 0.466 | 1.862 |
| TSFC, kg/N-hr | 0.069 | 0.099 |

It is evident that the extraction of power to drive the fan reduces the core jet velocity. The lower jet velocities substantially reduce the turbofan engine thrust for the same size inlet and total engine mass flow rate. Thus the high-bypass-ratio turbofan is less likely to be used for military applications requiring high speed and therefore high thrust per unit of frontal area. This is reflected in the specific thrust based on total engine mass flow. On the other hand, the specific thrust based on core mass flow shows that a significant increase in thrust can be achieved by adding a fan to an existing turbojet design. The major advantage of the fanjet is shown in the fuel flow rate and TSFC comparisons, where the superior fuel economy of the fanjet appears.

The success of the turbofan or ducted-fan engine has made it clear that further advances in jet engine fuel economy are possible with higher bypass ratios. The large-diameter cowlings necessary for drastic increases in turbofan bypass ratio, however, appear impractical. Still, advances in propeller technology now make flight at high subsonic Mach numbers possible with gas-turbine-driven unducted fans.

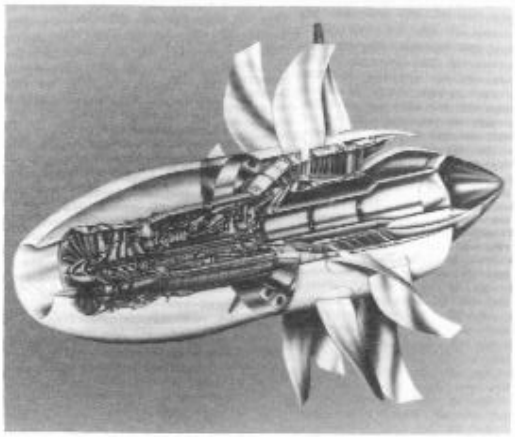

**FIGURE 9.32** UDF® engine allows higher bypass ratios than ducted turbofan engines. (Courtesy of GE Aircraft Engines.)

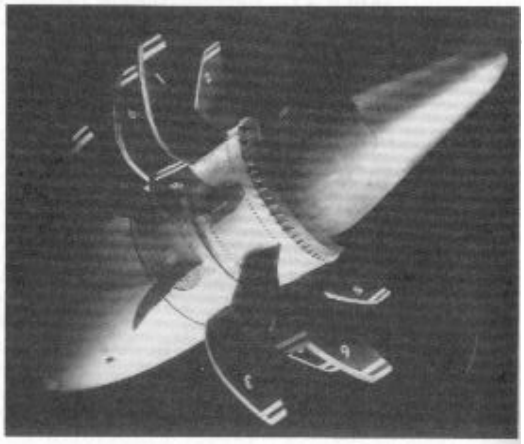

**FIGURE 9.33** UDF® engine. (Courtesy of GE Aircraft Engines.)

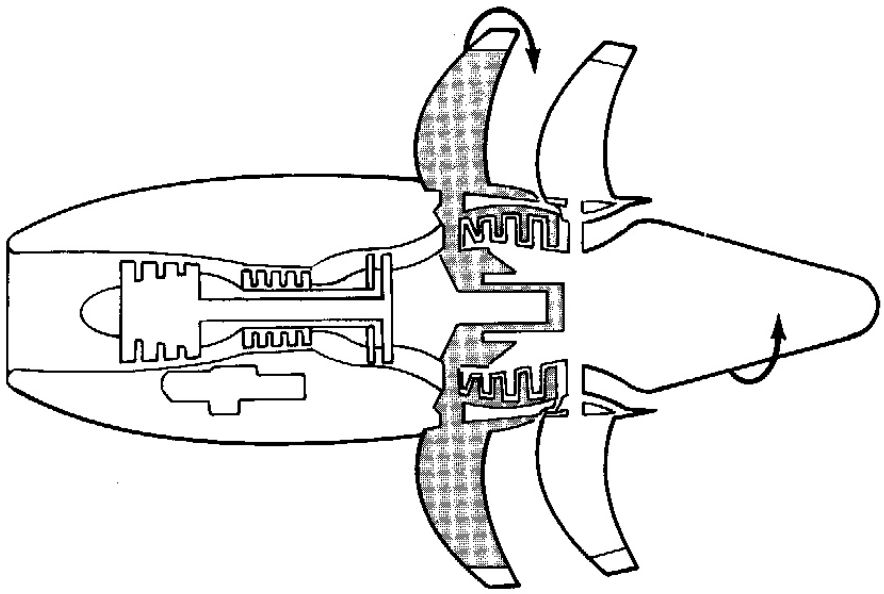

**FIGURE 9.34** Schematic diagram of UDF® engine showing contrarotating fan design. (Courtesy of GE Aircraft Engines.)

Figures 9.32 and 9.33 show a UDF®* engine featuring contrarotating fans installed in an engine nacelle. A twin-spool gas generator upstream of the fans supplies combustion gas to the cantilevered fan section. In this design the forward fan blades are coupled directly to the outer fan-turbine blades, as shown in Figure 9.34, and rotate clockwise. The free-wheeling aft fan section, which includes the

* UDF® is a registered trademark of General Electric Co., U.S.A..

inner fan-turbine blades, rear fairing, and tailcone assembly, is cantilevered at the rear of the engine and rotates counterclockwise.

With unducted-fan engines, very high bypass ratios are possible. The UDF engine, with an overall pressure ratio of approximately 42 at top of climb, has demonstrated substantial SFC reductions over modern turbo fans, approximately 20% lower than the best of the current turbofan engines. In-cabin noise, originally expected to be a problem with unducted fans, was very low–equal to or less than that of today's turbofan-powered aircraft (ref. 55).

Despite the attractiveness of the unducted fan concept, it appears that in the next decade large transport aircraft will use ducted fans that incorporate more modest increases in bypass ratio together with increases in overall pressure ratio for improved performance. Reference 63, for example, anticipated the family of 75,000 to 95,000 pounds-thrust turbofans coming into use around 1995. They were expected to have a bypass ratio of 9 and overall pressure ratio about 45 to give a 9% improvement in SFC over then-existing engines. The reference anticipated that the engines would have a low speed, low pressure ratio fan for low noise. The fans were expected to be made of composite materials to save about 25% weight over competing metal fans.

**Bibliography and References**

1. Curran, Paul F., "Clean Power at Cool Water," *Mechanical Engineering*, Vol. 109, No. 8 (August 1987): 68-71.

2. Grover, Ralph W., et al.; "Preliminary Environmental Monitoring Results for The Cool Water Coal Gasification Program." Proceedings of the EPRI Sixth Annual Conference on Coal Gasification, Palo Alto, Calif., October 15–16, 1986.

3. Watts, Donald H., Dinkel, Paul W., and McDaniel, John E., "Cool Water IGCC Performance to Date and its Future in the Electric Utility Industry," U.S. Utility Symposium, Palm Springs, Calif., October 1987.

4. Gluckman, Michael J., et al., "A Reconciliation of the Cool Water IGCC Plant Performance and Cost Data with Equivalent Projections for a Mature 360-MW Commercial IGCC Facility." Cool Water Gasification Program, October 1987.

5. Fahrion, M. E., "Materials Development Experience at Cool Water Coal Gasification Plant." Cool Water Coal Gasification Program, October 1987.

6. Anon., "Boilers and Auxiliary Equipment," *Power*, June 1988: 91–229.

7. Ehrlich, Shelton, "Fluidized-Combustion Boiler Technology–1988 Update." Missouri Valley Electric Association Engineering Conference, Kansas City, Mo., March 1988.

8. Ehrlich, Shelton, "Fluidized Combustion: Is It Achieving Its Promise?" Electric Power Research Institute, Palo Alto, Calif.

9. Pollak, Robert, "Status of First U.S. CAES Plant," *EPRI Journal*, December 1988: 49–52.

10. Allison, P. R., and Berman, P. A., "PACE 260 at Comanche, the First Two Years." ASME Gas Turbine Conference, ASME Paper 76-GT-109, 1976.

11. Anon., "Upgraded Combined Cycle Will Save Over $6 Million per Year in Fuel," *Gas Turbine World*, May–June 1968: 13–18.

12. Bammert, K. and Groschup, G., "Status Report on Closed-Cycle Gas Turbines in the Federal Republic of Germany." ASME Gas Turbine Conference, ASME paper 76-GT-54, 1976.

13. Williams, Robert H., and Larsen, Eric D., "Aeroderivative Gas Turbines for Stationary Power," *Annual Review of Energy*, Vol. 13 (1988): 429-489.

14. Anon., "The Purpose of PURPA," *Mechanical Engineering*, August 1988: 56.

15. Henneforth, James C., and Todd, Douglas M., "Cogeneration on a Large Scale," *Mechanical Engineering*, August 1988: 51-53.

16. Anon., "Modular Cogeneration: A Capital Idea," *Mechanical Engineering,* August 1988: 54-57.

17. Diamant, R. M. E., *Total Energy.* New York: Pergamon Press, 1970.

18. Horlock, J. H., *Cogeneration: Combined Heat and Power*. New York: Pergamon Press, 1987.

19. Williams, R. H., "Industrial Cogeneration," *Annual Review of Energy*, Vol. 3, 1978: 313-356.

20. Clarke, E. L., "Cogeneration, Efficient Energy Source," *Annual Review of Energy*, Vol. 11, 1986: 275-294.

21. Joskow, P. L., "The Evolution of Competition in the Electric Power Industry," *Annual Review of Energy*, Vol. 13, 1988: 215-238.

22. Larson, E. D., and Williams, R. H., "Steam-Injected Gas Turbines," *ASME Journal of Engineering for Gas Turbines and Power*, Vol. 109, January 1987: 55-63.

23. Burnham, J. B., Giuliani, M. H., and Moeller, D. J., "Development, Installation, and Operating Results of a Steam-Injection System (STIG) in a General Electric LM 5000 Gas Generator," *ASME Journal of Engineering for Gas Turbines and Power*, Vol. 109 (July 1987): 257-262.

24. Boutacoff, David, "Pioneering CAES for Energy Storage," *EPRI Journal*, January-February 1989: 31-39.

25. Pollak, Robert, "Status of First U.S. CAES Plant," *EPRI Journal*, December 1998: 49-52.

26. Anon., "The Circulating Fluidized Bed Boiler," *Heat Engineering*, Foster Wheeler Corp., September-December 1986: 88-89.

27. Anon., "A Combined-Cycle Cogeneration Plant," *Heat Engineering*, Foster Wheeler Corp., January-April 1986: 67-73.

28. Douglas. John, "Quickening the Pace of Clean Coal Technology," *EPRI Journal*, January-February 1989: 5-15.

29. Clarke, Ed, "Cool Water Coal Gasification Program: An Update," *EPRI Journal*, September 1988: 45-48.

30. Johnson, Gordon L., "Tailoring Controls to Accomodate Circulating Fluidized Bed Boilers," *Power*, May 1989:72-73.

31. Kolp, D. A., and Moeller, D. J., "World's First Full STIG LM5000 Installed at Simpson Paper Company," *ASME Journal of Engineering for Gas Turbines and Power*, Vol. 111 (April 1989): 200-210.

32. Scalzo, A. J., et al., "A New 150-MW High-Efficiency Heavy-Duty Combustion Turbine," *ASME Journal of Engineering for Gas Turbines and Power*, Vol. 111 (April 1989): 211-217.

33. Cohn, Art, "Steam-Injected Gas Turbines Versus Combined Cycles," *EPRI Journal*, October-November 1988: 40-43.

34. Holway, Donal K., and Moody, Joe R., Jr., "Salina Pumped Storage–Design and Operating History," *Waterpower '83*, Proceedings of the International Conference on Hydropower, Vol. 2, 861-870, 1983.

35. Anon., "Pumped Storage," Engineering Foundation Conference, American Society of Civil Engineers, 1975.

36. Barrows, H. K., Water Power Engineering. New York: McGraw-Hill, 1934.

37. Douglas, John, "Tools of the Trade for Hydro Relicensing," *EPRI Journal,* July-August 1988: 4-13.

38. Holway, Donal K., Private Communication, June 21, 1989.

39. Makansi, Jason., "Ultralow Emissions, Performance Tied to Process Knowhow," *Power*, June 1989: 64-66.

40. Bretz, Elizabeth A., "Examine Full Impact of Injecting Steam into Gas Turbine Systems," *Power*, June 1989: 53-61.

41. Brunner, Calvin R., *Handbook of Hazardous Waste Incineration*. Blue Ridge Summit, Pa: Tab Books, 1989.

42. Spiewak, Scott A., *Cogeneration and Small Power Production Manual*, 3rd ed. Lilburn, Ga.: Fairmont Press, 1991.

43. Weston, Kenneth C., "Turbofan Engine Analysis and Optimization Using Spreadsheets," Proceedings of the ASME Computers in Engineering Conference, August 1, 1989.

44. Cohen, H., Rogers, G. F. C., and Saravanamuttoo, H. I. H., *Gas Turbine Theory*, 3rd ed. New York: Longman, 1987.

45. Wilson, David Gordon, *The Design of High-Efficiency Turbomachinery and Gas Turbines*. Cambridge, Mass.: MIT Press, 1984.

46. Chenoweth, C. V., Schreiber, H., and Dolbec, A. C., "20 Years of Operation at Horseshoe Lake Station–Oklahoma Gas and Electric Company," Procedings of the American Power Conference, Vol. 96, 1984.

47. Roll, Mark W., "The Dow Syngas Project," *Turbomachinery International*, Vol. 32, No. 1, January-February 1991: 28-32.

48. Larson, E. D., and Williams, R. H., "Biomass-Gasifier Steam-Injected Gas Turbine Cogeneration," *ASME Journal of Engineering for Gas Turbines and Power*, Vol 112, April 1990: 157-163.

49. Zaugg, P., and Stys, Z. S., "Air-Storage Power Plants with Special Consideration of USA Conditions," *Brown Boveri Review*, Vol. 67 (December 1990): 723-733.

50. Kehlhofer, Rolf, *Combined-Cycle Gas and Steam Turbine Power Plants*. Lilburn, Ga: Fairview Press, 1991.

51. United Technologies Turbo Power and Marine Systems, Inc. FT8 Gas Turbine Brochure.

52. Goldstein, Gina, "Rechanneling the Waste Stream," *Mechanical Engineering*, Vol. 111 (August 1989): 44-50.

53. Butler, Arthur J., and Hufnagel, Karl R., "Skagit County Resource Recovery Facility Design of a 2500-kW Waste-to-Energy Plant," ASME '89–JPGC/Pwr-12, October 1989.

54. Douglas, John, "Beyond Steam," *EPRI Journal*, December 1990: 4-11.

55., G.E. Aircraft Engines source, personal communication.

56. Riley, Shaun T., (manager of LM 5000 and Industrial programs, G. E. Marine and Industrial Engines & Service Div.), personal communication.

57. Riley, Shaun T., "STIG Increases Output from Aeroderivative Gas Turbines," *Modern Power Systems*, June 1990: 41-47.

58. Stewart, Norman, "Shell Coal Gasification," *EPRI Journal*, June 1989: 38-41.

59. Sundstrum, David G., "Status of the Dow Syngas Project: Three Years of Experience at the World's Largest Single Train Coal Gasification Plant," Proceedings of the American Power Conference, Vol. 52, 1990, pp. 512-515.

60. Anon., "Gasifier Demo Heralds New Era for Gas Turbines," *Power*, October 1989: S-24–S-28.

61. Anon., "Cogen System Balances Steam Cycle Demand," *Power*, October 1989: S-42–S-44.

62. Ullman, Ronald R., and Duffy, Thomas J., "Integrated Material and Energy Recovery from Municipal Solid Waste," Proceedings of the American Power Conference, Vol. 52, 1990, pp. 570-577.

63. Smith Jeffrey J., " The GE90 ... When is Big' Big Enough?" ASME Turbo Expo–Land, Sea, and Air, Orlando, Fla., June 6, 1991.

64. Lamarre, Leslie, "Alabama Cooperative Generates Power from Air," EPRI Journal, December 1991: 12-19.

65. United States Department of Energy website, www.fe.doe.gov.

66. Schroeter, Jeffrey W., "The Merchant Revolution," *Mechanical Engineering Power*, May, 2000.

67. Lane, Jon, "More Power, Fewer Players," *Mechanical Engineering Power*, May, 2000.

## EXERCISES

9.1 A 10-MW gas turbine operating at the conditions in Example 5.1 exhausts through a process heat exchanger, with the combustion gas leaving at 200°F. What is the rate of heat transfer to the process? If the heat transfer is to liquid water, what flow rate of water can be increased in temperature from 50°F to 160°F in the heat exchanger? How many homes with an average heating demand of 60,000 Btu/hr could be serviced by the gas turbine in a district heating application where there is a 20% energy loss in the system distributing heat to the customers? What is the unweighted system energy utilization factor?

9.2 Design the combustion gas heat exchanger required in Exercise 9.1. Indicate the type selected, the required surface area, the geometric configuration, and overall size.

9.3 The oxygen remaining in the exhaust gas of a 5-MW gas turbine supplies the oxidizer for a process heater that burns methane completely. The gas turbine operates at the conditions of Example 5.1. What is the nominal heat transfer rating if the heater is designed for an exit temperature of 300°F? What is the rated of fuel consumption and the unweighted energy utilization factor of this combined heat and power system? What would the maximum heater output be if the gas turbine were shut down and atmospheric air were supplied to the heater with the same supplemental fuel firing rate?

9.4 Compare the unweighted energy utilization factors for the simple-cycle and regenerative gas turbines of Examples 5.1 and 5.2, assuming their exhausts serve unfired process heat exchangers with 250°F exit gas temperatures. Compare the energy utilization factors, assuming the useful heat in each is weighted by the cycle's thermal efficiency.

9.5 The exhaust of a 2-MW gas turbine, operating at the conditions of Example 5.1, transfers heat to an absorption chiller with a COP of 0.78. The exhaust gas leaves the chiller at a temperature of 220°F. How many tons of refrigeration can be produced by the chiller? What is the unweighted EUF based on shaft power and chiller rate of cooling?

9.6 A 20-MW simple-cycle gas turbine operates with compressor inlet conditions of 101 kPa and 15°C, a turbine inlet temperature of 1200°C, and a compressor pressure ratio of 12. The compressor and turbine isentropic efficiencies are 84% and 88%, respectively. The turbine exhaust flows through a process heat exchanger and exits to the atmosphere at 110°C. Determine the gas turbine cycle state properties, the thermal efficiency, and the work ratio, accounting for an 80-kPa pressure drop on the process heat exchanger gas turbine exhaust side. What is the rate of heat transfer to the process through the heat exchanger? If the heat transfer is to liquid water, what flow rate of water can be boiled at atmospheric pressure if water enters the heat exchanger at 30°C? How many homes with an average heating requirement of 20 kW can be heated in a district heating application where there is a 15% loss in the distribution of heat to customers? What is the unweighted system energy utilization factor?

9.7 Design the combustion gas heat exchanger required in Exercise 9.6. Indicate the type selected, the required surface area, the geometric configuration, overall size, and the estimated pressure drops. Can you improve significantly on the assumed heat exchanger pressure drop used in Example 9.6?

9.8 The exhaust of a 5-MW gas turbine supplies the oxidizer for a heater that burns methane completely. The gas turbine operates the 101 kPa and 15°C compressor inlet conditions and 1060K turbine inlet temperature. The engine has compressor and turbine isentropic efficiencies of 86% and 88%, respectively, and a compressor pressure ratio of 10. What is the nominal heat transfer rating of the heater? What is the total rate of fuel consumption and the unweighted energy utilization factor? Combustion gases leave the heater at 200°C.

9.9 The exhaust of a 2-MW gas turbine operating at 960°C turbine inlet temperature with a compressor pressure ratio of 9 transfers heat without loss to operate an absorption chiller with a COP of 0.83. The exhaust gas leaves the chiller at a temperature of 120°C. The compressor inlet conditions are 105 kPa and 25°C, and the compressor and turbine isentropic efficiencies are 82% and 86%, respectively. How many tons of refrigeration can be produced by the chiller?

9.10*Develop a spreadsheet like that in Table 9.1, and investigate the influence on the combined-cycle efficiency of varyingeach of the following:
(a) HRSG exit temperature.
(b) Steam turbine throttle temperature.
(c) Gas turbine inlet temperature.
(d) Compressor pressure ratio.

9.11 A closed-cycle gas turbine using air as a working fluid has an intercooler, a reheater, and a recuperator. The overall pressure ratio is 6. The low-pressure compressor has a pressure ratio of 2. Both compressors are driven by the high-pressure turbine. All turbomachines are 85% efficient. Compressor inlet temperatures are 80°F, and turbine inlet temperatures are 1500°F. Regenerator effectiveness is 75%.
(a) Draw T-s and flow diagrams, and label both compatibly.
(b) Identify actual temperatures, in degrees Rankine, at all stations of significance.
(c) If the low-pressure compressor inlet pressure is 6 atm, what are the intercooler and reheater gas pressures?
(d) Calculate the total compressor work, and compare with the work for a single compressor with 85% efficiency without intercooling.
(e) What is the gas turbine net work?
(f) What is the total external heat addition?
(g) How much heat is available from the precooler for district heating ?
(h)What is the plant thermal efficiency?
(i) What is the plant energy utilization factor if 80% of the precooler heat rejection is used for district heating?
(j) If the turbines deliver 100MW of power, what is the air flow rate and
(k) the rate of consumption of coal, in tons per hour (12,000 Btu/$lb_m$ heating value and 90% combustion efficiency)?

---

* Exercise numbers with an asterisk involve computer usage.

9.12 A closed-cycle gas turbine using air as a working fluid has an intercooler, a reheater, and a recuperator. The overall pressure ratio is 6. The low-pressure compressor has a pressure ratio of 2. Both compressors are driven by the high-pressure turbine. All turbomachines are 85% efficient. Compressor inlet temperatures are 15°C, and turbine inlet temperatures are 1000°C. Regenerator effectivenesss is 75%.
(a) Draw T-s and flow diagrams, and label both compatibly.
(b) Identify actual temperatures, in degrees Kelvin, at all stations of significance.

(c) If the low-pressure compressor inlet pressure is 6 atm, what are the intercooler and reheater gas pressures?
(d) Calculate the total compressor work, and compare with the work for a single compressor with 85% efficiency without intercooling.
(e) What is the gas turbine net work?
(f) What is the total external heat addition?
(g) How much heat is available from the precooler for district heating?
(h) What is the plant thermal efficiency?
(i) What is the plant energy utilization factor if 80% of the precooler heat rejection is used for district heating?
( j) If the turbine delivers 100 MW of power, what is the air flow rate and (k) the rate of consumption of coal in kilograms per second (25,000 kJ/kg heating value and 90% combustion efficiency)?

9.13 Starting with the selected combined-cycle design for Example 9.1, consider a modification to the heat-recovery steam generator that allows saturated liquid water at state 12 to be extracted for industrial process use. Assume that the water is returned to the condenser as a saturated liquid at the condensing temperature. Assume that process use dictates the mass flow rate extracted, with the balance of the water going as steam to the steam turbine. Calculate and tabulate the heat supplied per unit of gas turbine mass flow as a function of the process liquid mass fraction of the total water flow entering the steam generator. Also calculate and plot the energy utilization factor as a function of the process mass fraction. If the gas turbine power output is 6 MW, what is the maximum saturated-liquid-water process heat transfer rate?

9.14* Starting with the selected combined-cycle design for Example 9.1, consider superheated steam at state 8 to be extracted for industrial process use. Assume that the water is returned to the condenser as a saturated liquid at the condensing temperature. Assume that process use dictates the mass flow rate extracted, with the balance of the steam created going to the steam turbine. Calculate and tabulate the process heat supplied per unit of gas turbine mass flow as a function of the process steam mass fraction of the water flow through the steam generator. Also calculate and plot the energy utilization factor as a function of the process mass fraction. If the gas turbine power output is 6 MW, what is the maximum superheated-steam process heat transfer rate?

9.15 Extend the analysis of Table 9.1 to include supplemental firing of the HRSG, to provide an inlet gas temperature of 1500°F and a steam turbine throttle temperature of 1000°F. Determine the influence of boiling temperature on the pinchpoint temperature difference, and on the net work per pound of gas turbine flow; and compare the combined-cycle thermal efficiency with the efficiencies of the individual cycles. Discuss the results of the analysis.

9.16 Extend the analysis of Table 9.1, to consider a modification of the heat-recovery steam generator that allows saturated water vapor at state 13 to be extracted for industrial process use. Assume that the water is returned to the condenser as a saturated liquid at the condensing temperature. Assume that process use of the steam has priority, with the balance of the steam going to

the steam turbine. Calculate and tabulate the process heat supplied per unit of gas turbine mass flow as a function of the process water mass fraction of the water flow through the steam generator. Also calculate and plot the energy utilization factor as a function of the process mass fraction. It the total power output of the combined cycle is 6 MW, what is the maximum process heat transfer rate?

9.17 Extend Exercise 9.15 to consider a modification of the heat-recovery steam generator that allows superheated steam at state 8 to be extracted for industrial process use. Assume that the water is returned to the condenser as a saturated liquid at the condensing temperature. Assume that process use of the steam has priority, with the balance of the steam going to the steam turbine. Calculate and tabulate the process heat supplied per unit of gas turbine mass flow as a function of the process steam mass fraction of the water flow through the steam generator for a boiling temperature of 600°F. Also calculate and plot the energy utilization factor as a function of process mass fraction. If the total power output of the combined cycle is 20 MW with no process heat, what is the maximum process heat transfer rate?

9.18 Design an open-cycle regenerative gas turbine cogeneration system in which a fraction of the turbine exhaust gas can bypass the heat exchanger for process use. Prepare a report stating your design criteria, defining your analysis methodology, and presenting performance data for the nominal design condition that you selected.

9.19 Perform the design required in Exercise 9.18, and include consideration of performance for a range of off-design process heat transfer requirements that are lower than the design value.

9.20 A 20-MW electric motor in a simple compressed-air-storage plant drives a compressor with a pressure ratio of 10 and an efficiency of 85% for six hours nightly. What power output can be obtained with a turbine inlet temperature of 1600°F if the plant operates for four hours during the day at constant power output? The turbine efficiency is 90%. What is the air-fuel ratio if methane is the fuel used? What is the net generation efficiency, considering only the fuel consumption of the turbine? Assume a daily cycle, that cavern pressure changes are negligible, and that the heat of compression is dissipated before generation begins.

9.21* An ideal steam turbine operates with 1000°F, 2000-psia throttle, and 1-psia condenser and produces 15 MW without extraction. When steam is extracted for process use at 500 psia, after use it is condensed to a saturated liquid at that pressure and throttled to the condenser. Tabulate and plot the process heating rate and the EUF as a function of extraction mass fraction.

9.22* A 25 MW steam turbine operates in 1000°F and 2000 psia with an efficiency of 87%. Eighty percent of the condenser heat transfer is used for an industrial process. Tabulate and plot the process heating rate and the EUF as a function of condenser pressure between 1 psia and 2 atmospheres.

9.23* Develop the equations and an algorithm for the analysis of the steam-injected gas turbine with an unfired steam generator producing superheated steam at the combustion chamber pressure and using methane as a fuel . Use the JANAF tables for thermodynamic properties of steam in the gas turbine. State clearly the assumptions made. Write a computer programming implementing the algorithm.

9.24 Consider a compressor operating at a pressure ratio of 20 and a polytropic efficiency of 86% that compresses ambient air at 101 kPa and 15°C into a cavern. Assume that heat losses from the cavern maintain the air at 15°C and constant pressure during the filling period from midnight to 6 am daily. The compressor is driven by a 20 MW electric motor. What is the daily mass addition to the cavern? From 2 pm to 6 pm daily the same mass of air that was added to the cavern during the night is heated to 1200K and allowed to escape to the atmosphere at a constant flow rate through a turbine expander with a 90% isentropic efficiency. What is the expander power output? What is the daytime energy output? What is the fractional fuel consumption reduction if a regenerator with 80% effectiveness is added to the system?

9.25 Resolve Example 9.2 for superheated steam injection at 400°, 500°, 600°, and 700°F and the combustor pressure level. Write a brief report on your findings on the influence of temperature of injected steam on STIG performance.

9.26* Use the STIG spreadsheet shown in Table 9.5 to verify the performance calculations of Figures 9.23 and 9.24.

9.27* Investigate the influence of compressor pressure ratio variation on STIG performance for the model of Example 9.2, and prepare a memo reporting your results.

9.28* Evaluate the separate influences of steam heat capacity and added mass on the thermal efficiency, power output, and work ratio for the model of Example 9.2.

9.29 Consider a two-shaft gas turbine to be modified for steam injection. The compressor pressure ratio is 9.3, and the turbine inlet temperature is 982°C. The isentropic efficiencies of the compressor and turbines are 83% and 90%, respectively. The gas generator mechanical efficiency is 99%, and the power turbine drives an electrical generator that has a 93% efficiency. Accounting for a 4% pressure loss in the combustor and a fuel heating value of 43,000 kJ/ kg, compare the electrical power output, specific fuel consumption, thermal efficiency, and fuel-air ratios for 0.0 and 0.05 steam-air ratios. Briefly described your selection of steam system design conditions.

9.30 It has been decided that the heat-recovery steam generator for a steam-injected gas turbine must be retubed to continue running it in the steam injection mode. The expected cost of retubing is $230,000. Steam injection produces an additional 4000 MW-hr per year, adding two cents per kW-hr to

revenue. What is the break-even operating time to recover the cost of this maintenance operation?

9.31 Compare the isentropic efficiencies of two compressors, each having a polytropic efficiency of 87% and pressure ratios of 6 and 18.

9.32 What is the polytropic efficiency of a turbine, with a pressure ratio 30, that has the same isentropic efficiency as a turbine having a polytropic efficiency of 92% at a pressure ratio of 12?

9.33* Compare the performance of a twin-spool turbofan engine with separate fan and compressor to that of a turbojet engine, both with an overall pressure ratio of 30 and a turbine inlet temperature of 1300K, and designed for an altitude of 15,000m and a flight speed of 275 m/s. The bypass ratio is 6 and the fan pressure ratio is 1.6. Assume turbine, fan, and compressor polytropic efficiencies of 90% and a combustor pressure loss of 3% of the compressor exit total pressure. Compare specific thrusts for engines built from the same core engine. Compare, also, specific fuel consumption and jet velocities.

9.34* Build a multicase spreadsheet for the conditions of Exercise 9.33, and use it to plot specific thrust and TSFC as a function of fan pressure ratio. Use the spreadsheet to explore further the influence of varying bypass ratio for a value of fan pressure ratio suggested by your plot. Write a memo discussing briefly the results of your study.

9.35 Develop an analysis for a turbofan engine, sometimes called an aftfan engine, in which the fan is located at the same axial station and directly attached to a low pressure turbine dedicated to driving the fan. The high-pressure turbine drives the compressor, and is located upstream of the fan. The compressor and fan each have their own separate inlets.

9.36 Express the work of a compressor in terms of its inlet temperature and pressure ratio using (a) the isentropic efficiency, and (b) the polytropic efficiency. Equate the relations, and solve for the compressor isentropic efficiency. Compare your result with Equation (9.13).

9.37 Express the work of a turbine in terms of its inlet temperature and pressure ratio using (a) the isentropic efficiency, and (b) the polytropic efficiency. Equate the relations, and solve for the turbine isentropic efficiency. Compare your result with Equation (9.10).